Monte-Carlo Based Pricing of American Options Using Known Characteristics of the Expected Continuation Value Function

Olle Ottander, Fredrik Lindstedt

Master's thesis
2022:E41

Lund University

Faculty of Engineering
Centre for Mathematical Sciences
Mathematical Statistics

Centrum Scientiarum Mathematicarum

Master's Theses in Mathematical Sciences 2022:E41
ISSN 1404-6342

LUTFMS-3445-2022

Mathematical Statistics
Centre for Mathematical Sciences
Lund University
Box 118, SE-221 00 Lund, Sweden

http://www.maths.lu.se/

Abstract

The problem of pricing American stock options is far more complex than pricing European options due to the possibility of early execution. This feature means that the decision to either hold on to the option or exercising it early must be continually evaluated, leading to closed form solutions such as the Black-Scholes Formula to not be applicable on American options written on dividend paying assets. In 2001, F. Longstaff and E. Schwartz developed a Monte Carlo-based pricing algorithm to handle this. The algorithm simulates a large number of stock price trajectories, evaluates the value of early exercise versus the expected value of holding on to the option using polynomial regression of the continuation value function at each time step and then values the option based on the optimal exercise times. However, this method does not utilize some known characteristics of the expected continuation value function such as convexity, non-negativity, an absolute value of its derivative not greater than 1, and decreasing or increasing depending on the option type. The aim of this thesis is to utilize these characteristics in the regression of the expected continuation value. Four different stock dynamic models are used to simulate the stock price trajectories - Black-Scholes, Merton Jump Diffusion, Finite Moment Log Stable and Heston dynamics. The model parameters are fitted to the market using non-linear least squares optimization. The pricing algorithm resulted in somewhat improved results, with estimates placed within the bid-ask spreads 39.2% of the time using the constraints compared to 35.8% without. The Finite Moment Log Stable stock dynamics performed best with an overall pricing accuracy of 54.9%. Finally, put options were overall more accurately priced than calls, possibly due to constant deterministic interest rates and computational complexities.

Preface

This paper is a master's thesis written in collaboration with the Division of Mathematical Statistics at Lund University during the spring of 2022.

We would like to thank Magnus Wiktorsson, our supervisor at Lund University, for his invaluable guidance in the field of continuous-time arbitrage theory and Monte Carlo statistics. His interest and enthusiasm in the two courses covering the theory inspired us to further explore the area.

Contents

1 Introduction

Financial derivatives are financial contracts where the value is derived from that of an underlying asset. While the value of the underlying asset may be observed, its relation to the derivative value might not be obvious. Determining a fair price for such a derivative may therefore involve estimation. Many kinds of derivatives exist on the financial market, with options being a common example. An option is a type of derivative that allows holders to either buy or sell an underlying asset to a given strike price at a certain maturity date. A contract that gives the holder the option to sell the underlying asset at the strike price is referred to as a put option, while a contract that allows the holder to buy the underlying asset is called a call option. If the contract can only be exercised on the maturity date, it is called a European option, whereas a contract that allows the holder to exercise it any time between the start and maturity date is referred to as an American option. There are also other types of options, such as Bermudan options, which allow the holder to exercise the contract at specific time points during the period before maturity. Options are financial instruments that allow for exposure to asset classes without owning the underlying asset, hedging against risk, and speculation. Common underlying assets which options are issued for include stocks, indexes, futures and currencies. In this report the focus will be on stocks, but much of the theory relates to options written on other assets as well.

While there exist models with closed form solutions for valuing European options, these can only find approximate solutions to American options. American options can instead be valued using numerical methods. This is because while a European option is only evaluated at its maturity date, an American option must be evaluated at all times in between the start and maturity date. The European option is a "point in time" instrument while the American option is a "continuous-time" instrument. Furthermore, as the value of owning an American option depends on when it would be exercised, the pricing of such an asset is complex and involves comparing the value of exercising versus the value of continuing to hold the contract, i.e. the expected continuation value, at an infinite number of points in time during the contract's validity. This expected continuation value, as a function of stock price, has some known characteristics such as convexity, non-negativity, increasing or decreasing for calls or puts respectively as well as having the absolute value of its derivative not greater than one.

In this thesis, the problem of valuing American options issued on stocks as the underlying asset is handled using Monte Carlo methods, which implies simulating a large number of stock trajectories over a certain time period and finding the arbitrage free option price based on these trajectories. There are many models describing the dynamics of a stock which can be used for these simulations, with Fischer Black and Myron Scholes' model from 1973 being the most famous example. Four models will be used in this report. These are the Black-Scholes, Merton Jump Diffusion, Finite Moment Log Stable and Heston model.

1.1 Problem Definition

The aim of this report is to price American stock options using a numerical Monte Carlo based approach while taking advantage of known characteristics of the expected continuation value function. This means simulating many different trajectories of future stock movements, determining optimal exercise time for each trajectory by comparing exercise value and estimated expected continuation value at each time step, and finally valuing the option's price using the optimal cash flows.

1.2 Previous Research

In 2001 Francis A. Longstaff and Eduardo S. Schwartz published the paper *Valuing American Options by Simulation: A Simple Least-Squares Approach* which describes a numerical method for pricing American options. The method discretizes the time period of the American option into a time grid, onto which multiple trajectories of the underlying asset are simulated. The value of the American option is then derived by stepping backwards through the time grid, at each step evaluating whether it is best to exercise or hold the contract, and keeping track of the optimal time for exercising. This results in a value for each trajectory representing its optimal exercise strategy. The value of the American option may then be estimated by taking an average of all trajectories' optimum values. In order to estimate the expected continuation value of holding on to the contract at a certain time step, a regression is performed, assuming a polynomial relationship between the price of the underlying asset and the value of continuation.

In order to estimate option prices, the stochastic dynamics of the underlying asset need to be modeled. There are many examples of previous research on these dynamics, with Black and Scholes' 1973 findings in collaboration with Robert C. Merton in the article *The Pricing of Options and Corporate Liabilities* pioneering the field of option pricing. Examples of other important research built on this theory that is used in this paper is Robert C. Merton's 1976 paper *Option pricing when underlying stock returns are discontinuous*, Steven L. Heston's 1993 paper *A Closed-Form Solution for Options with Stochastic Volatility with Applications to Bond and Currency Options* and finally Peter Carr's and Liuren Wu's 2003 paper *The Finite Moment Log Stable Process and Option Pricing*.

1.3 Research Aim

The report aims to continue on the work of Longstaff and Schwartz by exploring a new approach to the estimation of the expected continuation value evaluated at each time step. Instead of simply assuming a polynomial relationship when performing the regression, the known characteristics of the relationship between expected continuation value and underlying stock price will be imposed. With hopes of improving the estimation of expected continuation value, this aims to give a more fair evaluation between exercising versus holding at all time steps, thereby giving a more accurate estimate of optimal exercise strategy and thus a more correct valuation of the option price.

Another aim of the report is to evaluate how the choice of model for simulating the underlying stock movement impacts the pricing of options. The four previously mentioned models will be analyzed, where their estimates and accuracy will be compared. By fitting the model parameters to the market, the models can be compared to find the one best suitable for mimicking real stock price movements.

1.4 Limitations

This report aims to evaluate techniques for pricing American options. The testing will be limited to options written on the Apple Inc. stock (AAPL) as the underlying asset. This also implies that the number of options to price is limited to the existing Apple options of different times to maturity and strike prices. Furthermore, data to evaluate is gathered from a single day in April (2022-04-08), thus observed stock and option prices are limited to those available on that day.

Furthermore, multiple assumptions have been made to facilitate computations. Fixed interest rate have been assumed in order for the stochastic processes to be time-invariant, thus significantly reducing computational time for pricing options of different maturities. Time of dividend as well as dividend amount as a percentage of share price are also modeled as deterministic constants in the approximation of dividends that may occur during the option's time to maturity.

2 Theory

2.1 Introduction to Option Theory

Suppose an option with a strike price of K and time of maturity T is written on a stock as an underlying asset. Further, let S_t denote the price at time t for this underlying stock. In the case of European options, the payoff may then be expressed as $\max(S_T - K, 0)$ for a call option and $\max(K - S_T, 0)$ for a put option. That is, the payoff of a European option only depends on strike price and the stock price at maturity, when exercising is possible. This payoff may be denoted $\Phi(S(T))$. For American and Bermudan options however, there exist many possible payoff expressions dependent on when the holder chooses to exercise the option. Like the European option, if τ denotes time of exercise, then the associated payoffs of a call or put option would be $\max(S_\tau - K, 0)$ or $\max(K - S_\tau, 0)$. For the Bermudan option, τ is limited to the potential exercise times defined by the contract, whereas for the American option, τ may be any time t between the start of the contract, t_0, and the time of maturity, T. A special case exists which is that of a call option written on non-dividend paying underlying stock, where theory states that early exercise is never optimal, implying that the payoff, and thereby also value, of European, Bermudan and American options should be equal.

2.2 Geometric Brownian Motion

A geometric Brownian motion (GBM) is a continuous-time stochastic process commonly used to model movements in the financial market, for example that of a stock price trajectory [1]. The logarithm of a geometric Brownian motion follows a Wiener process with drift. It can be expressed as a stochastic differential equation (SDE) defined as:

$$dX_t = \alpha X_t dt + \sigma X_t dW_t \tag{1}$$

$$X_0 = x_0 \tag{2}$$

where W_t is the Wiener process. A Wiener process is defined by the following properties:

1. $W_0 = 0$
2. For $t > 0$, every increment $W_{t+u} - W_t, u \geq 0$ is independent of past values of W_t
3. Increments are normally distributed with mean 0 and standard deviation $\sqrt{u}$: $W_{t+u} - W_t \sim \mathcal{N}(0, \sqrt{u})$
4. W_t is continuous in t

The GBM displayed in Equations 1 and 2 has two terms - a locally deterministic drift $\alpha X_t dt$ and an additive Gaussian noise term $\sigma X_t dW_t$, where α is known as the *drift term* and σ is known as the *diffusion term*. In general, stochastic differential equations are extremely complicated to solve. The geometric brownian motion is a special case where, using the Itô formula, a closed form solution can be found.

When defining the Itô formula, a process X is defined with a stochastic differential given by $dX_t = \mu_t dt + \sigma_t dW_t$ where μ_t and σ_t are adapted processes. Another process Z_t is then defined as $Z_t = f(t, X_t)$ where f is a $C^{1,2}$-function. The Itô formula then states that Z_t has a stochastic differential given by

$$df(t, X_t) = (\frac{\partial f}{\partial t} + \mu_t \frac{\partial f}{x} + \frac{1}{2}\sigma_t^2 \frac{\partial^2 f}{\partial x^2})dt + \sigma_t \frac{\partial f}{\partial x} dW_t \tag{3}$$

To find a solution to the geometric Brownian motion X_t formulated in Equation 1, the process $Z_t = \ln(X_t)$ is first defined. Applying the Itô formula on this process and utilizing the fact that $[dW_t]^2 = dt$ as Δt tends to 0, its stochastic differential can be expressed as

$$\begin{aligned} dZ_t &= \frac{1}{X_t} dX_t + \frac{1}{2}(-\frac{1}{X_t^2})[dX_t]^2 \\ &= \frac{1}{X_t}(\alpha X_t dt + \sigma X_t dW_t) + \frac{1}{2}(-\frac{1}{X_t^2})\sigma^2 X_t^2 dt \\ &= (\alpha dt + \sigma dW_t) - \frac{1}{2}\sigma^2 dt \end{aligned}$$

which results in Z_t having the stochastic differential

$$dZ_t = (\alpha - \frac{1}{2}\sigma^2)dt + \sigma dW_t \tag{4}$$

$$Z_0 = \ln(x_0) \tag{5}$$

As there is no Z_t in the right-hand side of Equation 4, it can be integrated into

$$Z_t = \ln(x0) + (\alpha - \frac{1}{2}\sigma^2)t + \sigma W_t$$

which also gives the solution to the geometric Brownian motion as

$$X_t = x_0 e^{(\alpha - \frac{1}{2}\sigma^2)t + \sigma W_t} \tag{6}$$

2.3 Black-Scholes

The Black Scholes model [2] is well known and describes the simplified price dynamics of an asset in the financial market. It is modelled using a geometric Brownian motion and is given by:

$$dB_t = rB_t dt \tag{7}$$

$$dS_t = \alpha S_t dt + \sigma S_t d\bar{W}_t \tag{8}$$

with S_t representing the stock price process and B_t the risk free price process (the bank account), where α, r and σ are deterministic constants and $\bar{W}_t$ is a Wiener process [1]. The bar denotes that the dynamics are defined under the real world probability measure P. Equations 7 and 8 represent the dynamics of a market with two instruments that are sufficient to price an option with the stock as an underlying asset. Now, an alternative probability measure Q is introduced with a market dynamic described by the following SDE:

$$dB_t = rB_t dt \tag{9}$$

$$dS_t = rS_t dt + \sigma S_t dW_t \tag{10}$$

The Q-measure is also referred to as the Martingale measure, as under it the stock price today equals the discounted expectation of the stock price tomorrow. This definition is also used to state a condition for an arbitrage free market, where a market model is said to be arbitrage free if and only if there exists a Martingale measure Q. The market dynamics under the Q-measure differs from those under the P-measure only in the expression of the stock price dynamics. Comparing Equation 8 and 10 one can see that the constant α is interchanged with the short rate r, and that the Wiener process $\bar{W}_t$ is interchanged with a Wiener process under the Q-measure, W_t. For the stock price process, it can be seen that it has r as its drift term and σ as its diffusion term.

Under the Q-measure, there exists a simple expression for the value of a European option. Let $\Pi(t;\Phi)$ be the price of a European call or put option, where Φ is the previously introduced payoff of the option. Furthermore, it is assumed that the price process Π only depends on the time t and the underlying stock process $S(t)$, i.e. that it may be expressed in terms of $F(t, S(t))$ where F is a smooth function. Then, the value of the European option at time t is

$$\Pi(t;\Phi) = F(t, S(t)) = e^{-r(T-t)}\mathbf{E}^Q_{t,s}\left[\Phi(S(T))\right] \tag{11}$$

which corresponds to calculating the expected value of the options payoff under the Q-measure, and discounting to time t with the discount factor $e^{-r(T-t)}$. This formula holds due to assumption of an arbitrage free market and thus the validity of the Q-measure.

For American or Bermudan options, the value is more complex, as the stopping time τ is not known at t. Instead, the value may be expressed as

$$\max_{\tau} \mathbf{E}^Q_{t,s}\left[e^{-r(\tau-t)}\Phi(S(\tau))\right] \tag{12}$$

where τ is the optimal exercise time for the contract. This implies that the valuation algorithm must not only determine the expected payoff, but also the optimal exercise time of the contract.

2.4 Other Models for Stock Dynamics

2.4.1 Merton Jump Diffusion Dynamics

The stock dynamics of the Merton Jump Diffusion model [9] is very similar to the dynamics of the standard Black-Scholes model. The difference is the addition of a stochastic jump variable on top of the stochastic diffusion. The idea is to take sudden asset price movements, both up and down, into account. The number of stochastic jumps per year follows a Poisson distribution, while the size of each jump is normally distributed. This results in the model's dynamics being represented in the following stochastic differential equation:

$$dS_t = rS_t dt + \sigma S_t dW_t + dH_t \tag{13}$$

where $H_t|N_t \sim \mathcal{N}(\mu_J N_t, \sigma_J\sqrt{N_t})$ with $N_t \sim Po(\lambda t)$ being the Poisson distributed number of jumps per year with λ as the expected number of jumps per year. The solution of the SDE is found using the solution of the geometric Brownian motion given in Equation 6. This results in, when letting z represent a standard Gaussian variable, the solution:

$$S_t = S_0 e^{(r-\frac{\sigma^2}{2}-c_H)t+\sigma W_t+N_j\mu_j+\sqrt{N_j}\sigma_j z}, \quad z \sim \mathcal{N} \tag{14}$$

Here, a notation c_H has also been introduced, representing a correction term used to keep the Martingale property of Black-Scholes despite the addition of the stochastic jump variable. Defining $c_H = \ln \mathbf{E}\left[e^{H_1}\right] = \lambda\left(e^{\mu_j+\sigma_j^2/2}-1\right)$ implies that $\mathbf{E}\left[e^{H_t-c_H t}\right] = 1$ for all t. Thus, the Merton model, like the Black-Scholes model, fulfill the Martingale property.

2.4.2 Finite Moment Log Stable Dynamics

The finite moment log stable (FMLS) model [3] was developed in 2003 with the aim of creating a model where the volatility smirk better mimics that which is observed in the financial markets. All three models previously discussed in this paper have their log-returns modeled using a Brownian motion. As the central limit theorem applies for these models, the volatility smirk flattens out very quickly as maturity increases. This is in contrast to what is commonly observed in the financial markets, where the existence of a volatility smirk implies a negative skewness with fat tails in the distribution of risk-neutral stock returns. To prevent such flattening, the FMLS model was created. The model's returns only has finite moments of the first degree and infinite moments for any order of two or greater, which means that the central limit theorem does not apply. The model can thereby fulfill the volatility smirk, and its associated negatively skewed and fat tailed risk-neutral return distribution, that is commonly observed in the financial markets. These negatively skewed and fat tails allow the FMLS model to be informally called a "crash model", as it efficiently handles the tendency for the market to develop relatively steadily as it grows in value and more drastically in financial declines.

This is implemented through the use of an α-stable Lévy process with maximum negative skewness. The process can divert from the Brownian motion used in the three previously used models through the parameter α, referred to as the tail index, which governs how negative the slope of the implied volatility smirk will be. With $\alpha = 2$, the choice of skewness will have no effect, there will be a flat volatility smirk, and the process will in fact be a Brownian motion. In this exception, the FMLS model in fact equals the Black-Scholes model. The tail index, α, is however allowed to take any values in $(1, 2]$, and a lower α corresponds to a steeper volatility smirk. This is illustrated in Figure 1, where implied volatility is plotted against moneyness, with moneyness being defined in [3] as $d = \ln(K/F)/\left(\sigma\sqrt{\tau}\right)$ where K is strike price, σ represents volatility of the underlying stock instrument, τ option term length, and F the corresponding futures price. As can be seen, as α decreases from 2 to 1.8, 1.5 and 1.2, the negative slope of the implied volatility smirk steepens. In addition to the tail index α, there is also the scale parameter σ which governs the width of the risk neutral distribution, in turn controlling the height of the volatility smirk. Despite the infinite return moments, the choice of maximum negative skewness gives finite price moments enabling option pricing.

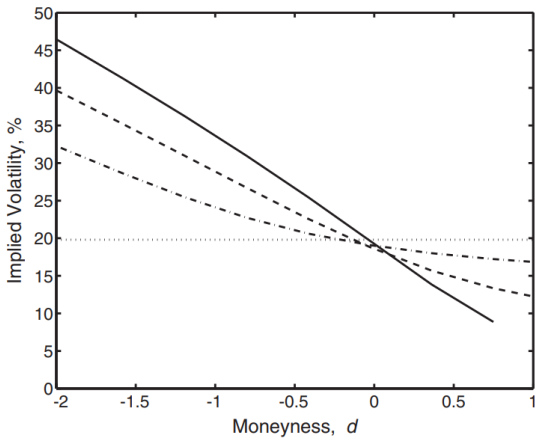

Figure 1: An illustrative plot of implied volatility against moneyness for a one month option, as the tail index α of the FMLS model varies from 1.2 (solid) to 1.5 (dashed), 1.8 (dashed-dotted) and 2 (dotted). Figure taken from [3] (CC-BY).

Summarized, the FMLS-dynamics models the stock movement as:

$$S_t = S_0 e^{(r+c)t+\sigma L_t^{\alpha,-1}} \tag{15}$$

where c is a correction term which ensures the Martingale property, and $L_t^{\alpha,-1}$ is the α-stable Lévy process with maximum negative skewness. The correction term c is defined by setting $\mathbf{E}\left[e^{ct+\sigma L_t^{\alpha,-1}}\right] = 1$ similar to in the Merton model, which gives $c = \sigma^\alpha \sec(\pi\alpha/2)$.

Adding to this model, this report will use an implementation of FMLS where a Brownian motion is added to better represent the dynamics of real stock movements. This means that the stock movement is given by:

$$S_t = S_0 e^{(r-\frac{\sigma_{BM}^2}{2}+c)t+\sigma_{BM}W_t+\sigma L_t^{\alpha,-1}} \tag{16}$$

2.4.3 Heston Dynamics

The Heston model [6], published in 1993, introduces stochastic volatility to the dynamics of the underlying asset. This is done to more realistically simulate the stock trajectories. The stock dynamics are consequently expressed by two stochastic differentials - one for the stock and one for its variance, where the stock's stochastic differential is as always dependent on its volatility, in this case expressed through the stochastic variance process V_t. These differentials are given by

$$dS_t = rS_t dt + \sqrt{V_t}S_t(\rho dW_{1t} + \sqrt{1-\rho^2}dW_{2t}) \tag{17}$$

$$dV_t = \kappa(\theta - V_t)dt + \beta\sqrt{V_t}dW_{1t} \tag{18}$$

where the two Wiener processes W_{1t} and W_{2t} have a correlation of ρ. Introducing these two differentials in the stock's stochastic differential allows the two processes dS_t and dV_t to have an arbitrary correlation of ρ. The variance will drift towards a long-run mean of θ, with its mean-reversion speed determined by another free parameter κ. The initial variance V_0 is set to σ^2 where σ is a parameter to the model.

2.5 Statistical Principles of Monte Carlo Estimation in Option Pricing

To price American options, numerical methods must be used. One such group of numerical methods are Monte Carlo methods, which is a group of numerical methods based on simulation and statistical analysis. By sampling many outcomes from an assumed probability distribution and utilizing statistical properties, one can mimic complex models and solve analytically difficult problems through estimation.

Let $X_1, ..., X_n$ be n identical and independently distributed simulations from the assumed distribution f, $h(X)$ the value to be estimated which depends on the random variable X, and

$\mu = \mathbf{E}[h(X)]$ be its expected value. Then, the expected value may be estimated through averaging as $n \to \infty$:

$$\hat{\mu}_{MC} = \frac{1}{n}\sum_{i=1}^{n} h(X_i) \to \int h(X)f(x)dx = \mu \tag{19}$$

This can be motivated by the strong law of large numbers, which states that the average of the i.i.d. random numbers X_i will almost surely converge to its expected value given that $|\mathbf{E}|[X_i] \leq \infty$. Furthermore, the central limit theorem gives insight into the variance of this estimate. Once again, let $X_1, ..., X_n$ be i.i.d. random variables with expected value μ and finite variance σ^2, with $\bar{X}$ denoting their average. Then, the random variable $T_n = \sqrt{n}\frac{\bar{X} - \mu}{\sigma}$ follows a standard normal distribution. Thus, the estimate obtained from the Monte Carlo method will approximately be normally distributed for large n [5].

2.6 Characteristics of the Expected Continuation Value

The expected continuation value function f, dependent on the underlying stock price, has the following known characteristics:

1. Non-negativity: $f(S_t) \geq 0$
2. (a) Call options
   Increasing: $S_{t_2} > S_{t_1} \Rightarrow \mathrm{f(S}_{t_2}) \geq f(S_{t_1})$
   (b) Put options
   Decreasing: $S_{t_2} > S_{t_1} \Rightarrow \mathrm{f(S}_{t_2}) \leq f(S_{t_1})$
3. Absolute value of derivative is not greater than one: $|\frac{df}{dS_t}| \leq 1$
4. Convexity: For all $0 \geq \lambda \geq 1$ and $S_{t_1} \neq S_{t_2}$, $f(\lambda S_{t_1} + (1-\lambda)S_{t_2}) \leq \lambda f(S_{t_1}) + (1-\lambda)f(S_{t_2})$

Figure 2 illustrates how an American call option's expected continuation value (in blue), i.e. the expected value of holding on to the option, and its exercise value (in red) is expected to vary with the underlying stock price. It illustrates how the expected continuation value is higher than the immediate exercise value for lower strike prices, and how the exercise value will surpass the expected continuation value at a certain point as the price of the underlying stock increases. The known characteristics of the function can also be seen in the figure.

The non-negativity of the expected continuation function can simply be explained by how an option can never have a negative value, as the cash flow it creates is either zero or greater than zero. For a call option, the expected continuation value is increasing with the underlying share price, as the immediate exercise value increases. The opposite holds true for put options. The function's absolute value of its derivative is never greater than one for a call option as it approaches the gradient of the exercise value line, but will never surpass 1, as a rise in share price can never imply a larger increase in expected continuation value than the increase in immediate payoff. Finally, the function is convex as the derivative continually increases without reaching 1 for call options and decreases without reaching 0 for put options.

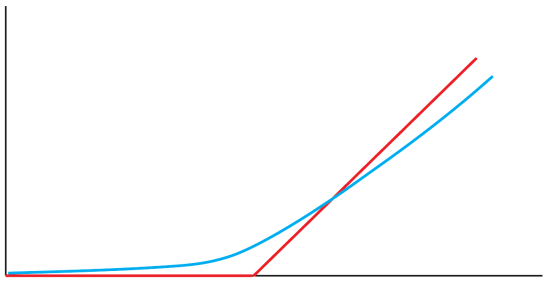

Figure 2: A example of an American call option's expected continuation value (blue) and exercise value (red) as functions of stock price

3 Method

This section will describe the various techniques used to simulate the trajectories of the underlying stock movements and how they are used to price the American options by stepping backwards in time from maturity to find the optimal exercise time. A simple method for incorporating dividend schemes into the pricing algorithm is discussed, as well as computational tricks for optimizing the algorithm's computational speed and how the various model parameters are fitted to mimic the dynamics of the real world financial market. Finally, the implementation of assumptions on the expected continuation value function is described.

3.1 Models for Stock Dynamics

Before running the pricing algorithm, trajectories for the underlying asset's price, and for one model also their volatilities, are simulated. Four different models for stock dynamics are used in this report. Below, their respective parameters and simulation formulas are detailed.

3.1.1 Black-Scholes

The Black-Scholes model for stock dynamics is a naive approach to an asset's price trajectory and has already been discussed in this paper. The main characteristics of the model are the constant and deterministic rate and volatility. The stock price's stochastic differential is given by Equation 10.

The numerical interpretation of the solution of the Black-Scholes stochastic differential equation is derived from the solution of the geometric Brownian motion formulated in Equation 6. α in this equation is exchanged for a risk-free r under the probability measure Q and σ_{BS} is an assumed constant volatility of the asset. The full stock price trajectory can then be simulated using a normally distributed variable to implement the noise related to the diffusion term. The trajectories are simulated using a numerical interpretation of Equation 6:

$$S_{k+1} = S_k e^{(r - \frac{\sigma_{BS}^2}{2})\Delta_t + \sigma\sqrt{\Delta_t} z} \tag{20}$$

where

S_k = stock price
r = risk-free rate
σ_{BS} = volatility of underlying stock
Δ_t = step size
$z \sim \mathcal{N}(0,1)$

3.1.2 Merton Jump Diffusion

The solution of the Merton dynamics SDE, given in Equation 14, has a numerical interpretation which is very similar to that of the Black-Scholes dynamics in Equation 20. With three additional terms representing the distribution of the stochastic jump process, and the previously discussed correction term $c_H = \lambda_{j_M}\left(e^{\mu_{j_M} + \sigma_{j_M}^2/2} - 1\right)$, it is given by:

$$S_{k+1} = S_k e^{\left(r - \frac{\sigma_M^2}{2} - \lambda_{j_M}\left(e^{\mu_{j_M} + \sigma_{j_M}^2/2} - 1\right)\right)\Delta_t + \sigma_M\sqrt{\Delta_t} z_1 + N_{j_k}\mu_{j_M} + \sqrt{N_{j_k}}\sigma_{j_M} z_2} \tag{21}$$

where

S_k = stock price
r = risk-free rate
σ_M = volatility of the Brownian motion
μ_{j_M} = mean jump size
σ_{j_M} = standard deviation of jump size
λ_{j_M} = jump intensity
Δ_t = step size
$N_{j_k} \sim Po(\lambda_{j_M}\Delta_t)$
$z_1, z_2 \sim \mathcal{N}(0,1)$

3.1.3 Finite Moment Log Stable

The FMLS dynamics given in Equation 16, including an α-stable Lévy process, is implemented using standard Gaussian and standard uniform variables, and trigonometric functions. The corresponding numerical implementation is given by:

$$\begin{aligned} S_{k+1} =& S_k e^{\left(r-\frac{\sigma_{b_F}^2}{2}+\sigma_F^{\alpha_F}\sec(\pi\alpha_F/2)\right)\Delta_t+\sigma_{b_F}\sqrt{\Delta_t}z_1} \\ & \times e^{(\Delta_t\sigma_F)^{1/\alpha_F}(1+\tan(\pi\alpha_F/2)^2)\sin\alpha_F(V+B)\left(\frac{\cos V-\alpha_F(V+B)}{W}\right)^{1/\alpha_F-1}/\cos V^{1/\alpha_F}} \end{aligned} \tag{22}$$

where

$$\begin{aligned} B &= \arctan(-\tan(\pi\alpha_F/2))/\alpha_F \\ V &= \pi(2z_2-1)/2 \\ W &= -\ln z_3 \\ S_k &= \text{stock price} \\ r &= \text{risk-free rate} \\ \sigma_{b_F} &= \text{volatility of the added Brownian motion} \\ \sigma_F &= \text{scale parameter for the volatility of the } \alpha\text{-stable Lévy process} \\ \alpha_F &= \text{tail index of the } \alpha\text{-stable Lévy process} \\ \Delta_t &= \text{step size} \\ z_1 &\sim \mathcal{N}(0,1) \\ z_2, z_3 &\sim U(0,1) \end{aligned}$$

3.1.4 Heston Model

The stock trajectories following the Heston dynamics are simulated using the following numerical solutions of Equations 17 and 18:

$$V_k = C \times \chi^2(d, V_{k-1}\lambda) \tag{23}$$

$$S_k = S_{k-1} \times e^{\Delta_t((r-\frac{\rho_H\kappa_H\theta_H}{\beta_H})+\frac{V_k+V_{k-1}}{2}(\frac{\kappa_H\rho_H}{\beta_H}-\frac{1}{2}))+\frac{\rho_H}{\beta_H}(V_k-V_{k-1})+\sqrt{\Delta_t\frac{V_k+V_{k-1}}{2}(1-\rho_H^2)}\times z} \tag{24}$$

where

$$\begin{aligned} d &= \frac{4\theta\kappa_H}{\beta_H^2} \\ \lambda &= \frac{4\kappa_H e^{-h\kappa_H}}{\beta_H^2(1-e^{-h\kappa_H})} \\ C &= \frac{\beta_H^2(1-e^{-h\kappa_H})}{4\kappa_H} \\ S_k &= \text{stock price} \\ V_k &= \text{variance} \\ V_0 &= \sigma_H^2 \\ r &= \text{risk-free rate} \\ \sigma_H &= \text{initial volatility of underlying stock} \\ \beta_H &= \text{volatility of variance} \\ \theta_H &= \text{mean reversion level of the variance} \\ \kappa_H &= \text{mean reversion speed of the variance} \\ \rho_H &= \text{correlation between stock price and variance} \\ \Delta_t &= \text{step size} \\ z &\sim \mathcal{N}(0,1) \end{aligned}$$

This simulation is not on an exact form, unlike previous models. To compensate for this, the number of steps per time unit is increased by a factor of 10 to reduce the simulation the error. However, after completing the simulation, only a tenth of the time steps are kept in order for the simulated path to be of the same form as the simulations of the other stock dynamic models.

3.2 Pricing the Option

The idea behind pricing an American stock option using Monte Carlo methods will here be illustrated through an example. The procedure is inspired by the works of Longstaff-Schwartz in their 2001 paper *Valuing American Options by Simulation: A Simple Least- Squares Approach* [8]. The main idea is to take backwards steps through the simulated stock trajectories starting at maturity, and at each time point comparing if the payoff is greater than the expected value of holding on to the option.

Suppose that there exists an American call option on an underlying stock, with price s_0 at time t_0, with strike price K and time to maturity T. Further, suppose n trajectories for the underlying stock between time t_0 to T has been generated through a stock dynamics model described in the previous section. Note however that when using Heston for modelling stock dynamics, some added complications follow which are described in Section 3.2.2. Then, let $S_{t,i}$ denote the stock price of the i:th trajectory at time t. Define time steps $t_0, t_1, ..., t_m$ of length Δt between time $t_0 = 0$ and $t_m = T$. These $m = T/\Delta t$ points of time form a discretization of the time line of the American option, allowing one to approximate the value of the option by evaluating whether exercising or continuing to hold the option is the optimal strategy at all possible steps of time.

The algorithm starts at the option's maturity. The exercise value of the call option at maturity for each trajectory is calculated through $\Phi(S_{T,i}) = \max(S_{T,i} - K, 0)$. A variable for optimal exercise time, τ_i is initiated as T together with a variable Φ_i^{opt} which represents the payoff of the option given an optimal execution at τ_i, which is initiated as $\Phi(S_{T,i})$. Then, one step is taken backwards in time. The exercise value at t_{m-1}, $\Phi(S_{t_{m-1},i})$, is calculated similarly and is now compared with the expected continuation value, i.e. the expected value of holding on to the option. The expected continuation value is estimated through a regression among the trajectories at t_{m-1}, where a relationship between the simulated continuation value, y, and current stock prices, x, of form $y = f(x)$ is assumed. Here, only in-the-money (ITM) trajectories are evaluated to save computing time, as the trajectories who are at-the-money or out-of-the-money (OTM) would not be exercised anyway. Data points are obtained for trajectory i by setting y_i to the value of Φ_i^{opt} discounted to the current time step t_{m-1}, and $x_i = S_{t_{m-1},i}$. The process of performing the regression is detailed in Section 3.2.1. Completing the regression allows one to calculate the expected continuation value for each trajectory through $f(x_i)$, which is then compared to the current exercise value. Trajectories for which the exercise value exceeds the expected continuation value are updated so that $\tau_i = t_{m-1}$ and $\Phi_i^{opt} = \Phi(S_{t_{m-1},i})$.

Then the process is repeated until t_0 is reached. That is, for a given time step t_q the algorithm:

1. Calculates $\Phi(S_{t_q,i}) = \max(S_{t_q,i} - K, 0)$ for all trajectories
2. Filters for in-the-money trajectories fulfilling $\Phi(S_{t_q,i}) > 0$. Defines y_i as Φ_i^{opt} discounted from τ_i to t_q with $x_i = S_{t_q,i}$, and regresses x_i onto y_i via $y_i = f(x_i)$ for these trajectories
3. Compares expected continuation value $f(x_i)$ with current exercise value $\Phi(S_{t_q,i})$ and filters for trajectories where $\Phi(S_{t_q,i}) > f(x_i)$
4. Updates $\tau_i = t_q$ and $\Phi_i^{opt} = \Phi(S_{t_q,i})$ for trajectories where exercise value exceeded expected continuation value to reflect that a new optimal exercise time has been found at t_q

When reaching t_0, the optimal exercise time and corresponding payoff value for each trajectory has been obtained. With the determined cash flows of the n trajectories, the value of the option is estimated through a final regression where all trajectories, both ITM and OTM, are used. This estimated continuation value is also compared to the exercise value at t_0 to check if payoff of instant exercise is greater than the approximated value. If so, the value of the option is instead given by the instant exercise payoff value.

3.2.1 Regression of the Continuation Value Function

In each step of the pricing algorithm, the expected continuation value as a function of current stock price is estimated through regression. This regression is performed through the Shape Language Modelling (SLM) toolbox in MATLAB, which is a toolbox that performs regression while imposing a set of specified characteristics onto the resulting curve [4]. These characteristics are chosen based on assumptions of how the expected continuation value should behave as a function of the underlying stock price, as detailed in Section 2.6. With the SLM toolbox, the criteria are imposed on a function of three degrees. The grid of stock prices are divided into different intervals, separated by 12 breakpoints referred to as knots, each with their own function being fitted. In Section 3.6, the choice of degree and number of knots will be investigated.

3.2.2 The Heston Case: Regression Over the Stock Price-Volatility Surface

The procedure for pricing an option described under 3.2 applies for when the underlying stock dynamics are modeled through Black-Scholes, Merton Jump Diffusion or Finite Moment Log Stable dynamics. However, in the case of Heston dynamics, the expected continuation value not only depends on a stochastic S_t, but also a stochastic V_t. Thus, the regression performed must be based on both features. This is approximated through bundling of the volatilities. At each time step, trajectories are grouped into n_g different clusters based on their current volatilities V_t. This corresponds to a simple grid bundling technique inspired by the 2015 report *The Stochastic Grid Bundling Method: Efficient pricing of Bermudan options and their Greeks* by Shashi Jaina and Cornelis W. Oosterleea [7]. While the grid bundling could be optimized through e.g. a k-means clustering algorithm, a simpler approach is here used. As the grid being bundled is only one-dimensional, the volatilities are simply grouped into equally large clusters of increasing size. Then, n_g different regressions are performed. For each of the n_g regressions, a representative V_t is chosen, chosen as the median value of the corresponding volatility cluster. Then, every trajectory is valued based on its two closest clusters. That is, a weighted combination of the evaluation from two most relevant regressed curves, where weights are determined based on distance to the representative middle element of the two clusters. In the most simple example, if one trajectory is exactly in between the two middle elements of two neighbouring clusters, the trajectory's expected continuation value would be estimated through evaluation in the two regressed curves and averaging.

3.3 Incorporating Dividends

To consider situations when the underlying stock issues a dividend during the contract timeline of an option, a simple feature is implemented in the pricing algorithm. First, all trajectories of S_t are simulated from t_0 to T. Also, let $d_{\%}$ be the dividend percent, i.e. the dividend payments size as a percentage of the stock price. Then, if a dividend takes place at time $t_d \in [t_0, T]$, the dividend amount $d = d_{\%} S_{t_d}$ is removed from all trajectories from t_d and onwards. That is, the update $S_t = S_t - d$ is performed for all $t \in [t_d, T]$.

3.4 Computational Optimization

Multiple techniques and tricks have been adopted to simplify testing and speed up evaluation. In this section, the adaptations made to enable the pricing of multiple strikes and maturities at once will be detailed.

3.4.1 Evaluating Multiple Strikes

To begin with, a linear property of the options value function has been utilized to allow for evaluation of many different strike prices at once. Let $f(t, S_t, T, K)$ be the value function of an american put or call option with underlying stock process S_t, maturity T and strike price K with initial value s_0. Let $S_{t+u} = S_t e^{X_{t+u} - X_t}$ be the development of the stock process between time t and $t + u$ for $u > 0$, where X represents a stochastic process such as those presented in 3.1. When $X_{t+u} - X_t$ is independent of S_t, which holds for all four models presented in 3.1, then the following property holds: $f(t, S_t, T, K) = K f(t, S_t/K, T, 1)$, i.e. the option's value function is linear in K. The process of valuing for multiple K at once is then implemented through initiating an $\hat{s_{0i}}$ for the $i = 1, 2, ..., n$ trajectories. Here, n different K_i are defined through evenly spaced placement in the interval of interest defined by the borders K_{min} and K_{max}. Then $\hat{s_{0i}} = s_0/K_i$ is formed. These initial values are then used as input in the stock dynamics modelling described in 3.1 and the pricing algorithm described in 3.2. When the pricing algorithm reaches its final iteration, at t_0, the n different $\hat{s_{0i}}$ values are used for the final regression. Then, the pricing of an option with a certain K^* can be estimated by evaluating the final regressed curve at $\hat{s_0}^* = s_0/K^*$ and multiplying the result with K^*.

3.4.2 Evaluating Multiple Maturities

Another computational technique used to increase the efficiency of the pricing algorithm is to value options with several different maturities at once. This is possible due to the assumed fixed interest rate, implying that the stochastic processes used are time-invariant. To facilitate this computation, the pricing of the different option's all start at the end of the simulated time period. Then, starting from t_0 suppose there are two time to maturities to be evaluated, T and $T_{1/3}$, where the latter time to maturity is a third of that of the first. Then, the pricing algorithm would as usual start

in the final time step corresponding to T and step backwards in time. Then, one third through the algorithm, as the time step corresponding to time $T - T_{1/3}$ is reached, the price of the option with maturity $T_{1/3}$ may be estimated. Then, the algorithm continues to step backwards until t_0 is reached, where the option with time to maturity T can be priced. Thus, a set of multiple maturities may be priced with no additional computational cost to that of the cost of pricing the option in the set with the longest maturity.

3.5 Empirical Evaluation

To evaluate the algorithm, outstanding options with observable markets prices will be used. Options with the Apple Inc. stock, with ticker AAPL, as underlying asset will be used, as these are some of the most traded options in the market. Defining t=0 as 2022-04-08, an initial stock value of $s_0 = 172.26$ (USD) is obtained [19]. From the Chicago Board Options Exchange, both put and call options with maturity at 2022-05-06, 2022-07-15, 2022-10-01, 2023-01-20 and 2023-03-17 are obtained [18]. 26 strike prices are selected, $100, 105, \ldots, 200, 210, \ldots, 250$ (USD). These data points are divided into a train and test data set. The train data set, used for finding suitable parameter values, uses 9 of the strike prices and maturities 2022-05-06, 2022-10-01 and 2023-03-17. The test set, used to evaluate the algorithm, uses 17 of the strike prices and the maturities 2022-07-15, 2022-10-01 and 2023-01-20. All strike prices and maturities of the two data sets are illustrated in Table 1.

		K																
Train	2022-05-06	100	115	130	145	160	175	190	210	250								
	2022-10-21	100	115	130	145	160	175	190	210	250								
	2023-03-17	100	115	130	145	160	175	190	210	250								
Test	2022-07-15	105	110	120	125	135	140	150	155	165	170	180	185	195	200	220	230	240
	2022-10-21	105	110	120	125	135	140	150	155	165	170	180	185	195	200	220	230	240
	2023-01-20	105	110	120	125	135	140	150	155	165	170	180	185	195	200	220	230	240

Table 1: Maturity date and strike prices, K, (USD) for the selected AAPL call and put options, divided into train and test data sets.

Translating the five maturity dates into times to maturity is done by counting the number of open market days between 2022-04-08 and the maturity dates [21]. Here, 252 market days per year is assumed. Thus, the maturity of 2022-05-06 translates to a time to maturity of $T_1 = 20/252$, 2022-07-15 translates to $T_2 = 67/252$, 2022-10-21 translates to $T_3 = 136/252$, 2023-01-20 translates to $T_4 = 198/252$ and 2023-03-17 gives $T_5 = 237/252$. For simulating the stock trajectories, 252 time steps per year is used, implying that the underlying stock trajectory is to be simulated 237 steps forward to enable the pricing of all maturities. For 100000 trajectories, the initial values $\hat{s_{0i}} = s_0/K_i$ are formed after linearly spacing K_i between $K_{min} = 90$ and $K_{max} = 275$ for trajectory $i = 1, 2, ..., 100000$.

To incorporate dividends that may occur during the times to maturity, Apple's dividend history is used. During the last 12 months, dividends were paid on 2021-05-13, 2021-08-12, 2021-11-11, 2022-02-07. These dividends all amounted to 0.22 USD per share [17]. Using $s_0 = 172.26$, a dividend percent of $d_\% = 0.22/172.26 = 0.13\%$ is defined. Assuming the same dividend dates for the next 12 months, the time to the dividends may be defined by counting the number of market days till the four calendar days. This gives four values for time to dividend, $t_{d1} = 22/252$, $t_{d2} = 84/252$, $t_{d3} = 151/252$, and $t_{d4} = 210/252$. At the corresponding time steps, the dividend amount d will be removed from the underlying stock price as detailed in Section 3.3.

3.6 Parameter Fitting

3.6.1 Stock Dynamics Parameters

The four different stock dynamic models all have a set of parameters whose values must be decided. The risk-free rate, r, present in all four models, is set to 0.0067 based on the 3-month US Treasury Bill rate observed before market opening on 2022-04-08 [16]. The remaining parameters are determined by solving a constrained optimization problem.

The optimization problem consists of pricing a set of put and call options with the four stock dynamic models, and comparing the obtained estimates with observed mid market prices with the aim of minimizing the absolute difference between the two. Here, the train data set with three

different maturities and 9 strike prices is used. The contracts and their market prices are shown in Table 2 and Table 3.

K \ T	**2022-05-06**	**2022-10-21**	**2023-03-17**
100	72.075	73.6	75.6
115	57.325	59.8	62.55
130	42.4	46.05	49.375
145	27.975	33.525	38.575
160	14.55	23.15	28.15
175	4.275	14.05	20.05
190	0.635	8.025	13.925
210	0.09	3.225	7.325
250	0.015	0.56	2.23

Table 2: Observed mid market prices for the set of call options used for parameter fitting (USD).

K \ T	**2022-05-06**	**2022-10-21**	**2023-03-17**
100	0.03	0.95	1.985
115	0.085	1.97	3.4
130	0.215	3.225	5.8
145	0.615	5.7	9.05
160	2.14	9.65	13.85
175	6.625	16.2	20.625
190	18.3	24.7	29.15
210	37.6	40.075	43.275
250	77.55	77.675	77.95

Table 3: Observed mid market prices for the set of put options used for parameter fitting (USD).

Running the pricing algorithm generates two 9x3 matrices with price estimates for the call and put options which are dependent on the parameter values used. Thus, denoting the vector of parameter values associated with a stock dynamics model as x, the obtained price estimate matrices may be denoted $C(x)$ and $P(x)$. Further, let the observed market prices in Table 2 and 3 be stored in two 9x3 matrices denoted C_{obs} and P_{obs}. Then, a loss value for the estimated prices is calculated by summing the absolute distance between each estimate and corresponding observed market price. This corresponds to the loss function:

$$L(x) = \sum_{i=1}^{9} \sum_{j=1}^{3} |C(x)_{i,j} - C_{obs\,i,j}| + |P(x)_{i,j} - P_{obs\,i,j}|$$

For a given stock dynamics model, the choice of parameter values is given by the solution to the optimization problem $\min_x L(x)$. Solving the problem is done with help of the MATLAB function *lsqnonlin*, which is a solver to nonlinear least-squares problems. To prevent the *lsqnonlin*-function to only find local solutions, the *MultiStart*-function is used to try several initiated values within the constraints in *lsqnonlin* [10]. This allows the optimization algorithm to explore a much larger area of the feasible region. 50 multistarts are used for all stock dynamic models except for the Heston model, where 30 were used, due to the large computational power needed for the Heston model.

This optimization is done for all four stock dynamic models, resulting in four sets of parameter values. Before solving the optimization problem, constraints and an initial value for each parameter is set. The four models parameters, with their constraints and initial values are shown in Table 4.

Black-Scholes	**Merton**	**FMLS**	**Heston**
Parameter *[Low. bound, upp. bound]* *(Initial value)*	*Parameter* *[Low. bound, upp. bound]* *(Initial value)*	*Parameter* *[Low. bound, upp. bound]* *(Initial value)*	*Parameter* *[Low. bound, upp. bound]* *(Initial value)*
σ_{BS} [0.05, 0.4] (0.25)	σ_M [0.05, 0.5] (0.25)	σ_{b_F} [0, 0.8] (0.1)	σ_H [0.05, 0.4] (0.2)
	μ_{j_M} [-0.5, 0.5] (0.3)	σ_F [0, 1] (0.2)	κ_H [0.5, 30] (10)
	σ_{j_M} [0.01, 0.9] (0.2)	α_F [1, 2] (1.8)	β_H [0.0025, 0.49] (0.04)
	λ_{j_M} [0.2, 5] (1.5)		θ_H [0.0025, 0.16] (0.04)
			ρ_H [-1, 0] (-0.6)

Table 4: Stock dynamics model parameters to be determined through parameter fitting, with constraints and initial values used.

3.6.2 Shape Language Modeling Parameters

For the regression performed via the Shape Language Modeling toolbox, there are two parameters to be fitted. The first is number of knots, which is the number of breakpoints used to separate the $\hat{S}_t$ grid into intervals where separate regressions are performed. The second is degree, which is the degree of the curve being regressed on each interval. The SLM toolbox allows three different choices of degree, 0,1 and 3, which corresponds to the resulting curve being piecewise constant, linear or cubic. Here, the choice of degree 1 and 3 is evaluated, together with the choice of number of knots being 6, 12, 18, 24 or 30. The evaluation will use the optimal stock dynamics model parameters obtained in Section 3.6.1, which were produced using a degree of 3 with 12 knots.

With the optimal model parameters, price estimates for the call and put options displayed in Table 2 and 3 may be obtained for different choices of degree and number of knots. Let the choice of values be represented by the parameter vector x_{SLM}. Furthermore, let $k = 1, 2, 3, 4$ represent the choice of underlying stock dynamics model, with $k = 1$ being Black-Scholes, $k = 2$ being Merton, $k = 3$ being FMLS, and $k = 4$ being Heston. Then the obtained 9x3 price estimates from using a model k may be represented by the matrices $C_k(x_{SLM})$ and $P_k(x_{SLM})$. Using the observed market prices C_{obs} and P_{obs}, a loss function for the obtained estimates from the different stock dynamic models is constructed as:

$$L(x_{SLM}) = \sum_{i=1}^{9}\sum_{j=1}^{3}\sum_{k=1}^{4} |C_k(x_{SLM})_{i,j} - C_{obs}| + |P_k(x_{SLM})_{i,j} - P_{obs}|$$

The optimal parameters are found by minimizing said loss function with respect to x_{SLM}.

4 Results

To evaluate the results of the attempted pricing of American stock options using Monte Carlo methods with assumptions on the expected continuation value function, the number of estimated option prices that are within the observed bid-ask spread is evaluated. The estimates are produced using parameters fitted to the market. Accuracy for the four models used will be presented and compared. The effect of the assumptions on the continuation value function made using the Shape Language Modeling toolbox is then evaluated by comparing the previous results to those obtained without making these assumptions.

4.1 Parameter Values Fitted to Market

The optimization problem detailed in Section 3.6.1 is run for all four stock dynamic models using constraints and initiated parameter values shown in Table 4. Solving the optimization problem results in the parameter values shown in Table 5. Interesting to note is the negative μ_{j_M} value in combination with the small σ_{j_M} value for the Merton model, implying that it may be classified as a crash model similar to the FMLS model. The obtained parameter values are used when producing the final pricing estimates presented in Section 4.2 and 4.3.

Black-Scholes	**Merton**	**FMLS**	**Heston**
Parameter *Value*	*Parameter* *Value*	*Parameter* *Value*	*Parameter* *Value*
σ_{BS} 0.2594	σ_M 0.1417	σ_{b_F} 4.7150e-04	σ_H 0.1959
	μ_{j_M} -0.3758	σ_F 0.1916	κ_H 4.2583
	σ_{j_M} 0.0107	α_F 1.6733	β_H 0.2901
	λ_{j_M} 0.6368		θ_H 0.1060
			ρ_H -0.8852

Table 5: stock dynamics model parameters to be determined through parameter fitting, with constraints and initial values used.

With the obtained stock dynamics model parameter values, the optimal parameter values for the SLM regression is evaluated using the loss function described in 3.6.2. The loss values for the different combinations of parameter values are shown in Table 6. It can be seen that there are five parameter combinations that perform best, all at a similar level. Overall, increasing the number of knots improves the loss value up until a certain point. However, for a degree of 3, more knots than 24 does not seem necessary. Similarly, for a degree of 1, more knots than 18 does not seem necessary. Limiting the number of knots is coveted as it reduces the number of regressions performed, resulting in a computationally less expensive algorithm. Furthermore, while increasing the number of knots could lower the bias of the estimates, it also risks increasing the variance of the estimates. Thus, either a degree of 1 with 18 knots or a degree of 3 with 24 knots seems best.

Choosing a degree of 1 over 3 is tempting as it reduces the computational cost per regression. However, upon evaluation of the pricing algorithm using a degree of 1, an unwanted linear behaviour was discovered among the prices of the options with shortest maturity that are close to being at the money, which can be seen in Figure 10. Thereby, a degree of 3 together with 24 knots is deemed to be the optimal parameter choice for the SLM regression. These are the parameters used when running the pricing algorithm in future sections.

Degree \Knots	**6**	**12**	**18**	**24**	**30**
1	782.67	305.08	233.96	231.73	237.25
3	926.29	375.01	268.21	229.54	235.00

Table 6: Loss function values for different degree and knots used in SLM regression.

4.2 Accuracy of Pricing

The four stock dynamic models used are evaluated by counting the number of estimated option prices that are within the observed bid-ask spread collected before market opening on 2022-04-08. Each model's accuracy is presented in Table 7. The estimated option prices used for these accuracy values are found in Tables 9 to 16 in the Appendix.

	2022-07-15	2022-10-21	2023-01-20	Total
BS				**23.5%**
Call	23.5%	5.9%	0.0%	9.8%
Put	41.2%	35.3%	35.3%	37.3%
Merton				**46.1%**
Call	47.1%	58.8%	35.3%	47.1%
Put	35.3%	41.2%	58.8%	45.1%
FMLS				**54.9%**
Call	41.2%	52.9%	11.8%	35.3%
Put	64.7%	76.5%	82.4%	74.5%
Heston				**32.4%**
Call	35.3%	52.9%	0.0%	29.4%
Put	41.2%	41.2%	23.5%	35.3%

Table 7: Share of options priced within ask-bid spread for four stock dynamic models, per maturity and option type.

The results vary greatly, from a 0% accuracy of the 9-month call option using Black-Scholes dynamics to an 88.4% accuracy of the 9-month put option using Finite Moment Log Stable dynamics. Overall, these two models are also the worst and best performing models respectively. In general, the crash models designed to take the possibility of a market crash into account, i.e. Merton Jump Diffusion and FMLS, perform significantly better than the other two. This is especially noticeable for the put options with longer maturities.

The pricing algorithm systematically undervalues certain options. Both the Black-Scholes and Heston model undervalues OTM put options as well as call options with longer maturities. Merton Jump Diffusion and FMLS instead undervalues OTM call options. This can be seen in Tables 9 to 16. A visual example can be seen in Figures 12 and 18 displaying the estimated call option prices found using Black-Scholes and Heston dynamics compared to the bid-ask spreads observed on the market. The estimated prices follow the curve of the bid and ask prices for longer maturities, but are all lower valued in comparison. This systematic error is greater the longer the maturity of the option. It is also greater for Black-Scholes than for Heston. The same behavior of the estimated prices can be seen for the put options. See Figures 20 and 17 in the Appendix.

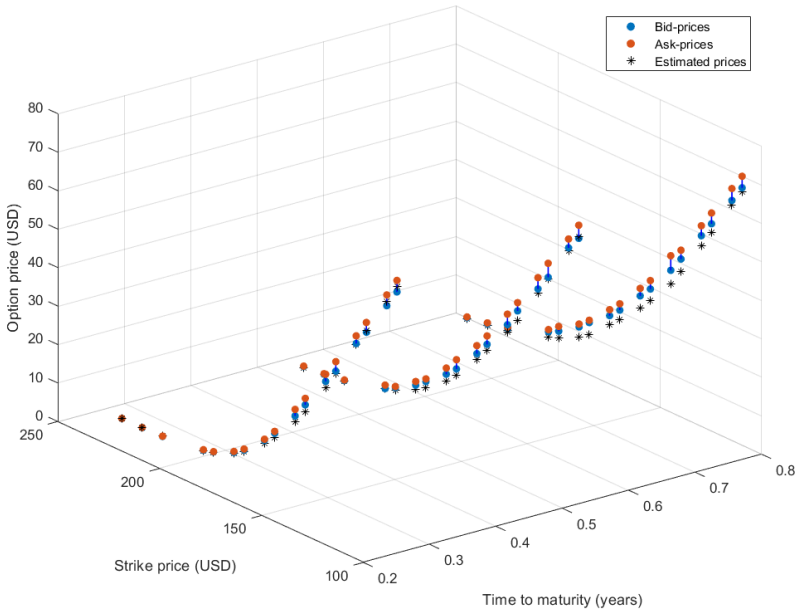

Figure 3: Estimated American call option prices using Black-Scholes stock dynamics compared to bid and ask prices observed on the market.

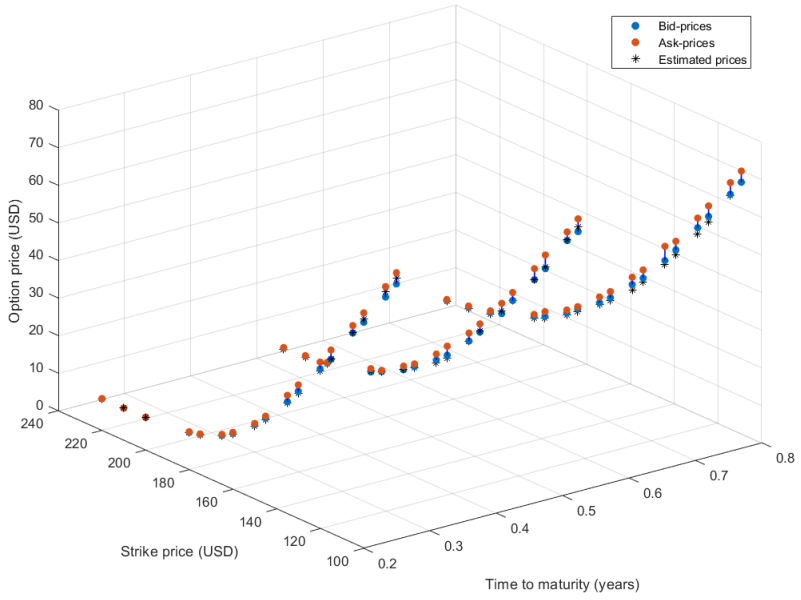

Figure 4: Estimated American call option prices using Heston stock dynamics compared to bid and ask prices observed on the market.

4.2.1 Model Specific Findings

The Black-Scholes dynamics provides a fairly good pricing accuracy of 37.3% for the put options, but performed significantly worse when pricing call options with an accuracy of 9.8%. Longer maturity call options had very low accuracies.

The Merton Jump Diffusion's simple addition of a Poisson-distributed number of jumps with normally distributed sizes greatly improved the accuracy compared to Black-Scholes with an overall pricing accuracy of 46.1%. This is mainly due to the model handling longer maturities better than Black-Scholes.

The Finite Moment Log Stable stock dynamics achieves the best results out of the four used in

this paper. It has an impressive 74.5% accuracy for the put options priced and is improved with longer maturities. Its pricing of call options are also good, with the exception of the longest call option maturity where only 11.8% of the options are priced within the observed bid-ask spreads.

Despite the stochastic volatility implemented in the Heston dynamics, its pricing accuracy of put options is very similar to that of the Black-Scholes dynamics. However, it is greatly improved for the call options, especially for the middle option maturity of 6 months from the date of observation. There is an abrupt drop in accuracy for the longest call option maturity.

4.3 Effect of Assumptions on Expected Continuation Value Function

The results in Section 4.2 were obtained using the assumptions on the expected continuation value function described in Section 3.2.1. The effect of imposing these assumptions will be evaluated here. The same pricing algorithm is run except for no assumptions being made when regressing the expected continuation value function. Table 8 shows the accuracy of the obtained estimates without using assumptions next to the estimates obtained in 4.2.

	Bid-ask accuracy		**Mean squared error**	
	Without assumptions	**With assumptions**	**Without assumptions**	**With assumptions**
Black-Scholes	24.5%	23.5%	7.782	7.897
Merton	45.1%	46.1%	3.429	3.483
FMLS	50.0%	54.9%	3.785	3.589
Heston	23.5%	32.4%	4.548	4.343
Total	**35.8%**	**39.2%**	**4.886**	**4.828**

Table 8: Share of options priced within the bid-ask spreads and the mean square error from the mid-price for four stock dynamic models, with and without assumptions on the expected continuation value function as part of the pricing algorithm.

In general, imposing assumptions on the expected continuation value function has a varied effect on the accuracy of the obtained option prices. The difference is most noticeable for the Heston stock dynamics, where an additional 9% of the options are priced within the bid-ask spread when the assumptions are enforced. The mean square error is also reduced from 4.548 to 4.343. For FMLS, the bid-ask accuracy is improved by about 5 percentage units and the mean square error is reduced from 3.785 to 3.589. For the Black-Scholes and Merton stock dynamics however, not using any assumptions yielded results with similar accuracy as when assumptions are used.

Although the estimates produced using assumptions are overall more accurate, plotting the two alternative estimates together illustrates how both produce a similar behavior for the option prices. As an example, Figure 5 illustrates the obtained prices for put options under the FMLS stock dynamics, both for the case of imposing assumptions and not doing so. Here, both estimates follow the shape formed by the bid-ask curves.

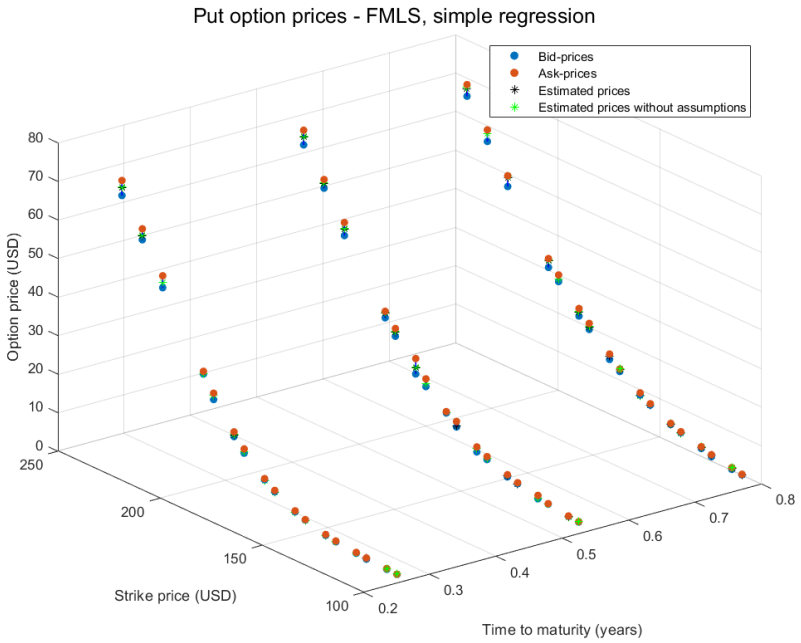

Figure 5: Estimated American put option prices using FMLS stock dynamics compared to bid and ask prices observed before market opening on 2022-04-08. Estimate achieved using assumptions on the expected continuation value function shown in black, estimates obtained without any assumptions are in green.

5 Discussion

5.1 Simulation of Stock Trajectories

5.1.1 Choice of Stock Dynamic Models

The four models used to simulate the stock trajectories in the Monte Carlo-based approach to option pricing provided varying results. The choice of these models is naturally of great importance when it comes to accurately pricing the American options, as they have different approaches to mimicking the movement of the AAPL stock. In the process of choosing appropriate models, they were considered with the aim of having competing models with different characteristics to be able to evaluate which are more suitable for the real options market.

The Black-Scholes model is of course the most simple of the four and was picked as a simple benchmark for the other models to be compared with. It was also used as a control for the pricing algorithm giving reasonable results when the more complex models were implemented in MATLAB. It is therefore not surprising that this performed the worst in its option pricing. The Merton Jump Diffusion model was chosen to explore the importance of the possibility of discontinuous jumps in stock price to mimic the expectations of the market reflected in the option prices. For that reason, it is interesting to note the large increase in accuracy for the Merton model compared to Black-Scholes. Models with stochastic jumps were expected beforehand to generally perform better, which is why the Finite Moment Log Stable model also was added as a more sophisticated option. The main purpose of the model is to purposely violate the central limit theorem to stop the volatility smirk from flattening out too quickly as maturity increases, which was a characteristic seen in the previously existing stock dynamic models but not in the options market. This important trait of the FMLS model provided excellent pricing accuracies for put options with longer maturities. Finally, all three of these models utilize a constant and deterministic volatility. The Heston model was therefore implemented to evaluate a model with stochastic volatility. This provided somewhat disappointing results, with only the call options with a time to maturity of 6 months being more accurately priced than when using Black-Scholes. Later in this section, it is discussed whether this might stem from non-optimal parameters being used for the Heston model.

5.1.2 Accuracy of Stock Trajectory Simulation

The four stock dynamic models all have the aim of simulating stock trajectories that mimic that of the AAPL stock. As has been previously mentioned in the report, various simplifications have been made to lower the computational cost of the pricing algorithm. This means that even after fitting the model parameters to fit real market data, the stock dynamics might still not be efficient enough to be used to price the options.

The constant and deterministic interest rate is likely the most important of these simplifications. Around the time the data was collected, there were wide expectations of the US Federal Reserve increasing the interest rates quickly within the coming year [15]. These expectations of the market will certainly have an effect on the option prices. In fact, increasing interest rates lead to increasing call option prices and decreasing put option prices [14]. This is because purchasing call options has the same potential for profit as purchasing shares of a stock, while an option purchase also frees up capital to be invested in the risk-free interest rate. A higher interest rate then implies a higher call option value. A similar comparison can be made between purchasing put options and short-selling, where short-selling enables the trader to invest the received capital in a risk-free rate while the purchase of a put options implies tying up capital in the amount of the put option price. The value of the put option will then decrease with an interest rate increase. These dynamics have not at all been accounted for in the pricing method.

Another simplification made which likely has a more minor effect on the pricing accuracy is the way the future dividend amount is decided in the algorithm. The dividends are paid out as a percentage of the current stock price, which means that small changes in stock price during the time period will also directly change the dividend payment. In reality, companies are pressured to provide a certain dividend amount to their shareholders. They are therefore not likely to decrease their dividend payment unless there are significant financial trouble in order to keep their dividend track record [13]. This error is however very small and not likely to be of major effect on the accuracy.

Finally, the discretization of time into one time step per day has varying effects for the different stock dynamic models. As mentioned in Section 3, Black-Scholes, Merton Jump Diffusion and FMLS are all implemented computationally to give exact solutions despite the discretization. However, the Heston dynamics are not. This was handled by simulating stock trajectories ten

times per day but only saving one of them, resulting in a slightly higher resolution in stock price simulation, reducing the simulation error somewhat. The error is however not removed completely.

5.2 Pricing Algorithm

While the pricing algorithm was developed based on the algorithm detailed by Longstaff-Schwartz in 2001, a number of considerations had to be made during the implementation which all impact the estimates produced by the algorithm.

5.2.1 Regression Using Only ITM Trajectories

Inspired by the Longstaff-Schwartz algorithm, only ITM trajectories were used in the pricing algorithm as the expected continuation value was regressed at all time steps to determine whether exercising or holding is optimal. The reason for this is that the trajectories that are not ITM would not be exercised, regardless of their current expected continuation value. Thus, the comparison would be unnecessary, and computing time could be saved by not regressing these trajectories. An exception to this rule is for time steps where final option prices are calculated. As detailed in Section 3.2, for the final evaluation of an option, the expected continuation value is regressed using all trajectories, as prices for both ITM and OTM options are to be evaluated. Illustrated in Figure 6 are two regressions, one made at t_1 and one at t_0. Here, the former only considers ITM trajectories while the latter includes all trajectories. As can be seen, restricting to ITM trajectories omits a large share of the available data points. Including all of these could impact the shape of the curve, and as a consequence also the estimations of the expected continuation value. In turn, this could have an effect on the judgement of optimal exercise time and the final price of the option being valued.

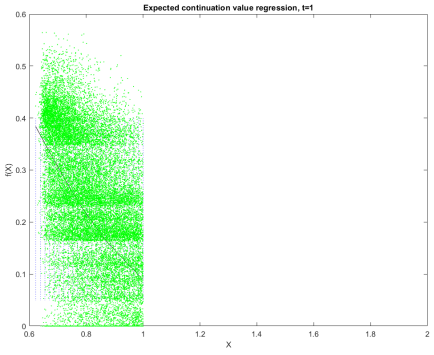

(a) The regressed curve at t_1. Only ITM trajectories are included in the regression. Data points in green and fitted curve in black. X represents $\hat{S}_{t_1}$ values and f(X) the expected continuation value.

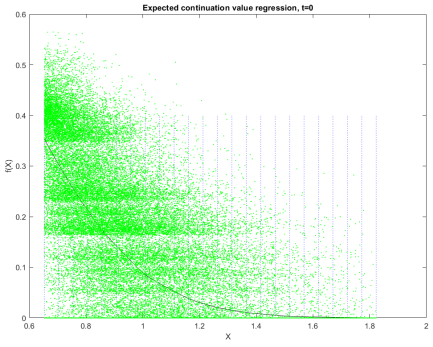

(b) The regressed curve at t_0. All trajectories, including those being ITM, ATM or OTM, are used in the regression. Data points in green and fitted curve in black. X represents $\hat{S}_{t_0}$ values and f(X) the expected continuation value.

Figure 6: Two regressions from the pricing algorithm, illustrating the difference between regressing ITM trajectories versus all trajectories.

5.2.2 Placement of Regression Knots

When regressing the expected continuation value function, the grid is divided into sub-intervals where separate regressions are performed. By default, the SLM toolbox separates the intervals by equally spaced knots. A second option offered by the toolbox is to let a nonlinear optimizer find the optimal placement of the knots. This would prevent the cases where the existence of outliers would lead to intervals that only contain a few data points, resulting in a poor regression on these subsections of the $\hat{S}_t$ grid. However, introducing this optimization yielded a serious increase in computational time, large enough to be considered not implementable given the available computational power in the fabrication of this report.

5.2.3 Regression for the Heston Model

For the special case of the Heston stock dynamics model, which has two stochastic processes S_t and V_t, the pricing algorithm had to be adjusted to take both into consideration. As detailed in Section

3.2.2, this was simplified by grouping the volatilities into sorted clusters, performing one regression per volatility cluster and evaluating the option prices based on a weighted combination of the two regression curves corresponding to volatility clusters closest the volatility of interest. Here, ten volatility clusters were defined, a number which could have been increased to allow for a more detailed bundling of the V_t grid space. Furthermore, a more complex approach to assigning the volatilities into clusters could have been implemented to minimize the effect of the simplification being made, as was mentioned briefly in Section 3.2.2. Instead of producing one regression per cluster and only using two of the regressions as part of the final valuation, a regression using the volatilities as an input to a function of expected continuation value given a fixed S_t could also have been made. In total, these measures could allow for an option valuation which more accurately represents the volatility of interest.

An interesting finding with the Heston parameters obtained in 4.1 is that they produce increasing volatilities due to the high value of the mean reverting parameter θ_H in relation to the initial variance of σ_H^2. In fact, upon producing the prices in the Results section, already 20 steps forward in time, there exists no variance trajectory whose value, V_{20}, is less than or equal to the initial volatility of σ_H^2. As a consequence, all prices evaluated inside the algorithm, i.e. the options with maturities 2022-07-15 and 2022-10-21, have been priced using the regression produced by the lowest volatility cluster, which does not properly represent the volatility of interest which is σ_H, as it is not present in this cluster. This implies that the produced prices are not quite reflecting the volatility which the options were to be valued in light of. While these parameter values were deemed as optimal based on the parameter fitting described in 3.6, it is possible that a stricter boundary on the parameter θ_H could have prevented this behaviour. It is also possible that the obtained parameter values were not optimal as is detailed in Section 5.3.5.

5.3 Parameter Fitting

While not being the main object of the study, the parameter values obtained in the parameter fitting of the stock dynamic models fill an important part of the work, as the obtained values greatly influence the obtained price estimates. In this section, the obtained values will be discussed in light of previous expectations and the outcomes reasonableness in relation to the actual financial markets which the study aim to reflect.

5.3.1 Black-Scholes

The only parameter fitted for the Black-Scholes model is the volatility σ_{BS}, where a value of 25.94% was obtained. The reasonableness of this parameter value may be judged in light of the VIX measure. The VIX is a volatility index measures by the CBOE and tracks the implied volatility of SP500 options [11]. On April 8th 2022, the index closed on 21.16 [20]. Given this implied volatility for the SP500 index, the obtained σ_{BS}, representing the implied volatility of the AAPL stock, seems reasonable.

5.3.2 Merton Jump Diffusion

For the Merton Jump Diffusion model, a σ_M value of 0.1417 was obtained. In addition to this, for the stochastic jump process, the parameter values $\mu_{j_M} = -0.3758$, $\sigma_{j_M} = 0.0107$ and $\lambda_{j_M} = 0.6368$ were obtained. This implies that in average once every $\frac{1}{\lambda_{j_M}} = 1.57$ years a jump will occur leading to an expected 37.56% decline of stock price. It is therefore declared a crash model. Observing the history of the AAPL stock, drops of around 30% has happened recently, although not in an instantaneous drop, rather between February and March 2020 as well as November and December 2021 [19]. Nevertheless, it is concluded that the obtained μ_{j_M} and λ_{j_M} are are not to be deemed completely misrepresenting of the real financial markets. The small σ_{j_M} does however seem unrealistic. Given the normally distributed jump sizes, this implies that more than 95% of all jumps that may occur would change the stock value between -35.5% and -40%. Furthermore, the likelihood for a positive jump to occur is practically non-existent. It seems unlikely that such a specific recurring jump size would exist for the AAPL stock. The fact that a positive jump is extremely unlikely to occur does also not seem representative of the real financial markets.

5.3.3 Finite Moment Log Stable

In the FMLS model, the parameter values obtained were $\alpha_F = 1.6733$, $\sigma_F = 0.1916$, and $\sigma_{b_F} =$ 4.7150e-04. Given the obtained α_F value, the stochastic α-stable Lévy process differs from a

Brownian motion, which has an α value of 2. It can then be viewed as a confirmation of Wu and Carr's hypothesis in the article introducing the FMLS model, which is that a Brownian motion is not sufficient in modelling the behaviour of an underlying stock price. Another interesting finding is the low σ_{b_F} value, representing the volatility of the separate Brownian motion which was added in addition to the α-stable Lévy process used in the original FMLS model. The low parameter value signals that adding an additional Brownian motion does not make up a vital part of the stochastic movement in the FMLS model in the scenario of this report. A reason might be that while the FMLS model may be considered as a jump process, most of its jumps are so small that it to an extent already resembles the movement of a Brownian motion.

5.3.4 Heston

Lastly, for the Heston model, the parameter values $\sigma_H = 0.1959$, $\kappa_H = 4.2483$, $\beta_H = 0.2901$, $\theta_H = 0.1060$, and $\rho_H = -0.8852$ were obtained. To begin with, the θ_H value indicates that the variance process will revert to a mean of 0.1060, corresponding to a volatility level of 0.326. Given the initial volatility value of $\sigma_H = 0.1959$, this implies that the volatility process will overall be increasing, as it drifts upwards towards the level of $\sqrt{0.1060} = 0.326$. This leads to a faulty volatility being used when estimating the option price for the two options with shorter maturities, as is discussed in Section 5.2.3. Also, it is interesting to note the ρ value which indicates a high negative correlation between the underlying stock price and volatility. The parameter was constrained to negative values in the interval $-1 < \rho < 0$ as there is a tendency for a stock's volatility to increase as its price declines, but a value of $rho = -0.8852$ indicates a very high negative correlation.

5.3.5 Validity of the Obtained Optimas

There is uncertainty whether the obtained parameters are optimal. To begin with, it is not certain whether the obtained optimal values truly are global optimums to the parameter fitting loss function, or only local. The *MultiStart*-function played an important role as it allowed for many initial values and thereby many local solutions to be evaluated. In general, more parameters being fitted implies a larger feasible region to be explored. While one can be quite confident in the obtained value of the single fitted parameter in the Black-Scholes model, the more complex models are less certain. This is especially true for the five fitted parameters of the Heston model, as this was not only the most complex model, but also the only model where 30 instead of 50 multistarts were used. With more computational time available, another optimal solution might have been found which could have resulted in a better pricing accuracy.

Additionally, a different choice of loss function could have produced a different set of optimal parameters. Instead of measuring the absolute difference from the mid price of the options in the train set, divergence from the bid-ask spread could have been measured. Another alternative could be measuring the distance from the mid price, but with less punishment for distance within the bid-ask spread. As the accuracy of the final pricing was judged based on how many estimates were inside the bid-ask spread, favouring predictions inside the spread might have been beneficial in training. Specifically, it might have prevented estimates that lie just outside the bid-ask spread.

5.4 Limitations of Accuracy Measure

The accuracy measure chosen for comparing the different models' pricing performances is binary, as an estimate can only be considered correct or incorrect depending on if it is placed within or outside of the bid-ask spread. This could potentially lead to unfair comparisons between models. An example is the accuracy value of 35.3% that is shared between both the call option priced using Merton Jump Diffusion and the put option priced using Black-Scholes, both options maturing on 2023-01-20. Despite the same accuracy, the estimations behave very differently, as can be seen in Figures 20 and 22. The Black-Scholes put options are systematically undervalued and are far from the observed option price for low strike prices, i.e. options far out-of-the-money. The Merton call option price estimations are however consistently closer to the observed prices with no apparent systematic error. An alternative accuracy measure is to instead consider the distance between estimate and mid-price. This was done using the mean square error in Section 4.3. This measure would possibly find the Merton call option more accurate than the Black-Scholes put. This measure would also match that of the measure used in the training phase during the parameter fitting. Akin to the reasoning in Section 5.3.5, matching the measure between the train and test phase could increase the obtained accuracy scores.

Another potential issue with the accuracy results is that the option price data was collected before market opening on 2022-04-08, which could lead to the bid and ask prices not being fully calibrated yet. The bid-ask spreads could then potentially be larger than what they would be when the market is open. This would then lead to higher pricing accuracies.

5.5 Possible Explanations for Systematic Undervaluation

5.5.1 The Effect of Constant Volatilities

The most prominent systematic undervaluation is that of the American call options priced using Black-Scholes stock dynamics, as was shown in Section 4.2. The most likely explanation for this is the tendency for options with longer maturities to have higher implied volatilities, as a consequence of a lengthier time leading to the stock price having a longer time period to move to a favorable price level [12]. Since the Black-Scholes model simulates the stock trajectories using a constant volatility, this will not be accounted for. The effect is then a systematic undervaluation of long-dated call options. A simple way to handle this would be to fit the parameters differently to each maturity, which would likely provide a higher volatility for the call options with longer maturities.

In Section 4.2 it can also be seen that the Heston model has less of a systematic undervaluation for these types of options than Black-Scholes. This is because the square root of the θ_H-parameter in the stochastic volatility process, signifying the mean-reversion level of the volatility, has a value of $\sqrt{0.1060} = 0.326$ which is greater than the volatility of the stock price process S_t of $\sigma_H = 0.1959$. This means that the volatility will increase over time. The fact that the Heston process still slightly undervalues longer call options means that this explanation does not fully resolve the error.

5.5.2 Impact of Crash Dynamics on Out-of-the-Money Put Options

Another notable systematic undervaluation is that of the out-of-the-money put options priced using Black-Scholes and Heston stock dynamics. The two main reasons for purchasing OTM put options is for hedging against a fall in stock price when one has a long position elsewhere as well as speculating in a coming bear market. This is because the value of the put option will of course increase as the stock price falls. The likelihood and sequent speculation of a sudden crash in stock prices will then lead to an increase of OTM put option prices. This is the dynamic that the two crash models used, i.e. the FMLS and Merton stock dynamics, handles more efficiently, as the more extreme falls in stock price will be accounted for in the pricing of put options far out-of-the-money. As a consequence, there is no systematic undervaluation for put options priced using FMLS and Merton dynamics.

5.5.3 American Options Simplified Into High-Frequency Bermudan Options

A simplification that will have a slight undervaluation effect on the option pricing of all four models is the discretization of time. Its effect on the stock trajectory simulation of the Heston dynamics has already been discussed, but it also has an impact on the pricing algorithm. American options will never be lower valued than European options as the holder in addition has the right to exercise the option at any point before maturity. Since time has been divided into one time step per day in this report, the holder is in effect only able to exercise the options at one specific point per day. This means that the exercise value in theory could have been higher at another point during the day. The evaluated options could be said to be of the Bermudan type.

This will always be a consequence of a numerical approach to option pricing, but could be minimized by increasing the number of time steps per day. This would also significantly increase the computational cost of the algorithm and require a very large RAM of the machine running it, which is why this was not done in this paper.

5.6 Put Option Prices More Accurate Than Calls

5.6.1 Computational issues

There are three difficulties with calculating the price of an American call option which may help explain the lower accuracy for calls compared to puts. To begin with, American call options with discrete dividends are, given a positive risk-free rate, theoretically only optimal to exercise just before a time of dividend or at the final time to maturity [1]. As a consequence, any options that were exercised early should have been exercised just prior to either $t_{d1} = 22/252$, $t_{d2} = 84/252$, or $t_{d3} = 151/252$, corresponding to an optimal exercise time step of 21, 83, or 150. In Figure 7, the

obtained optimal exercise times for the 100000 trajectories used when pricing a call option with maturity 2023-01-20 using Black-Scholes dynamics are illustrated. As can be seen, while there are clusters of trajectories around the time steps leading up to 83 and 150, these are not the only times where the trajectories have been exercised. It is then concluded that the algorithm does not follow this theory, which may partly explain the relatively poor accuracy for calls.

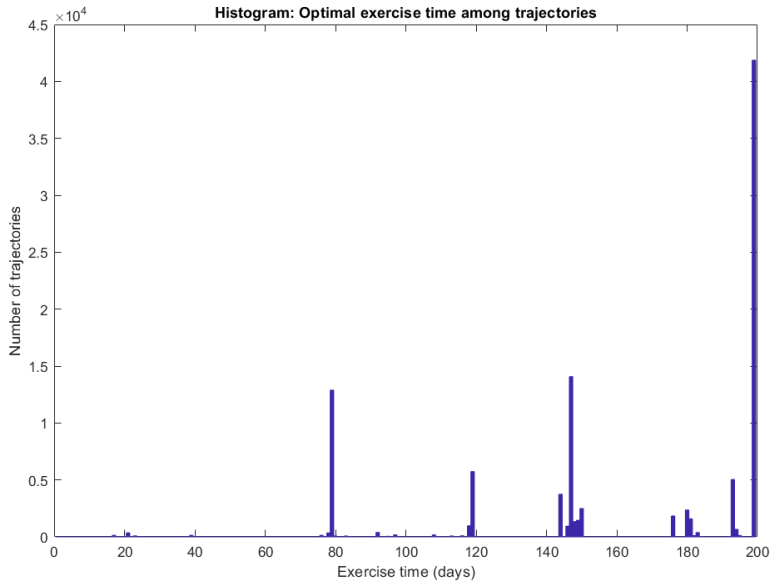

Figure 7: Histogram over deemed optimal exercise time for 100000 trajectories when pricing a call option using Black-Scholes stock dynamics.

Moreover, an error in the algorithm relating to the dividends may amplify this effect. In the implementation detailed in Section 3.4.2, allowing multiple maturities to be evaluated in a single run, time invariance was assumed. However, the discrete dividends are not time invariant and as such will occur at different times for the different maturities. By earlier reasoning, pricing the call option is more sensitive to the timing of the dividends and as such, this may also help explain the lesser accuracy of the call options compared to the put options. The small relative size of the dividends may limit this effect though.

Lastly, the interval for regression differ between put and call options. For puts, when filtering for ITM trajectories, the input to the regression, $\hat{S}_t$, is bounded by 0 and 1. For calls however, the input is only bounded from below by 1. This means that the regression used in the pricing algorithm is always done over a compact area for puts, whereas for the calls the regression is done over a area with no upper limit. This means that outliers may have a bigger impact on the pricing of call options. This could also explain some of the difference between the accuracy of call prices compared to put prices.

5.6.2 Market reasons

An interesting pattern that can be seen in the accuracy values of Table 7 is that estimated put option prices are more accurate than call option prices for the longest maturity option in all four models. One important explanation for this is the fact that constant risk-free interest rates were used in the simulation of the stock trajectories. This decision was made to enable time-invariant stock dynamics, allowing for the simulation of options with different maturities at once. Sadly, the timing of this simplification could hardly have been worse with the previously mentioned market expectations of rapid interest rate increases by the US Federal Reserve in April 2022. This would lead to increased call option prices and decreased put option prices as a result of market speculation. Since these effects have not been accounted for, all models used in the pricing algorithm will have undervalued the call options and overvalued the put options. Now, in combination with the systematic undervaluation as a result of the constant volatilities for all models except Heston, the pricing of Bermudan options and not American options as well as the lack of crash dynamics for Black-Scholes and Heston, the put option price estimations will be pushed back into the correct bid-ask spreads, while the call option estimations will instead be pushed further away.

The difference in put and call option estimate accuracy is even greater for the two crash models, Merton and FMLS, than for the other two. One possible explanation for this is that in the cases of a sudden crash in stock price, the put option greatly increases in value while the call option greatly decreases in value. For the Merton Jump Diffusion model, this type of crash will happen in average once every 1.57 years and lead to a 37.56% decline of stock price in average. This is a fairly unlikely event that will have large impacts on both put and call prices. For longer maturities, the probability of such an event increases, leading once again to increased put option estimates and decreased call option estimates. Similarly as for the constant interest rate, the estimates will be pushed towards or further away from the bid-ask spreads respectively.

5.7 Varied Effect of Assumptions in Regression

While the estimates obtained with assumptions are more accurate, where 39.2% instead of 35.8% of the options are priced in the bid-ask spread, the behavior of the estimated prices is similar and resembles that of the bid-ask prices for both alternatives. A reason for this may be that the nature of the pricing formula may alone often already capture the desired behaviour of the expected continuation value function which the assumptions enforce. As an example, Figure 8 shows the expected continuation value regression performed at time step 150 for a put option, both with and without enforcement of assumptions. As can be seen, both curves demonstrate the desired behaviour, as they are non-negative, decreasing, convex and have a maximum derivative whose absolute value is not greater than 1. Rather, it seems to be mainly for early time steps, where the existence of outliers among the simulated stock trajectories is more frequent, that the assumptions may come into play. Figure 9 shows the same regression but at time step 4. It illustrates how the resulting curve of the regression performed without assumptions does not follow the wanted behavior for the stock trajectories whose values are outliers. As can be seen, the curve produced without assumptions behaves strangely in its leftmost part. There are even a few parts of the curve where moving further to the right yields an increase in value. This implies that an increase in the underlying stock value would increase the put option price, which is a behaviour that one would not expect in the financial markets. In these cases, the curve where the assumptions were enforced is clearly preferable. This may explain the slight effect that imposing assumptions has on the resulting accuracy of the price estimates. It is worth noting that placing the knots using an optimizer, as detailed in Section 5.2.2, could prevent the unwanted unstable behavior of the regressed expected continuation value, which could limit the role of the enforced assumptions.

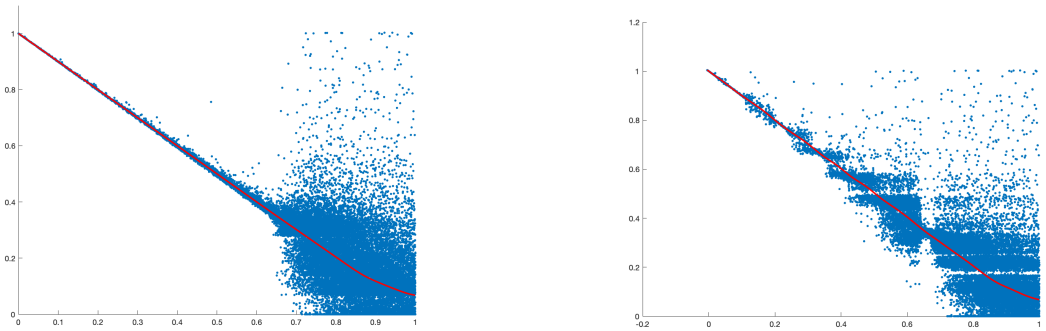

(a) Regressed curve at time step 150 for a put option when assumptions are enforced.

(b) Regressed curve at time step 150 for a put option when no assumptions are enforced.

Figure 8: Regressions from the pricing algorithm, at time step 150, illustrating how the fitted curves demonstrate a desirable behavior, regardless of whether has been enforced.

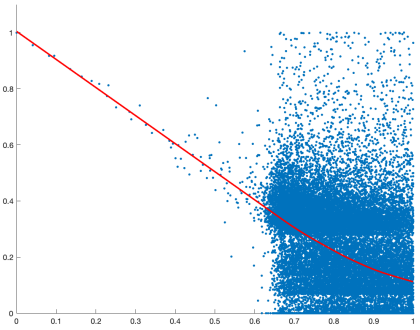

(a) Regressed expected continuation value for a put option at time step 4 when assumptions are enforced.

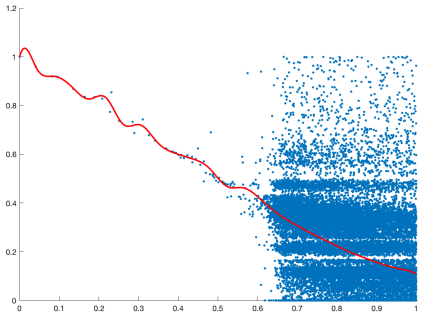

(b) Regressed expected continuation value for a put option at time step 4 when no assumptions are enforced.

Figure 9: Regressions from the pricing algorithm, at time step 4, illustrating how forcing assumptions onto the expected continuation value function impacts the shape of the regressed curve. The effect is mainly limited to the part of the $\hat{S}_t$ grid made up of outliers.

6 Conclusion

The hypothesis of an improved accuracy in the Monte Carlo based pricing algorithm developed by Longstaff-Schwartz in 2001 using assumptions on the expected continuation value function was a success. The developed algorithm using assumptions on the expected continuation value function acheived an overall pricing accuracy of 39.2%, compared to 35.8% when no assumptions were used. While the regression on the expected continuation value generally followed its known characteristics without imposing assumptions, some cases were observed were enforcing these assumptions fixed clear violations.

As expected, the Black-Scholes model resulted in the lowest total pricing accuracy of 23.5%. Surprisingly, the Heston dynamics followed thereafter with a pricing accuracy of 32.4% despite its stochastic volatility. The Merton Jump Diffusion and FMLS stock dynamics were the most efficient models in the pricing of American options with accuracies of 46.2% and 54.9% respectively thanks to the possibility of sudden crashes in stock price. This shows the importance of the crash dynamic in modelling stock price trajectories.

There was a fairly dramatic systematic undervaluation of option prices using the developed Monte Carlo-based algorithm. There are many possible explanations for this, where an important one is that the volatilities fitted to the market were adjusted for all three maturities at once, despite that the Implied Volatility has a tendency to increase for longer maturities. The crash dynamics of Merton Jump Diffusion and FMLS was also found to create an undervaluation effect among OTM put options. However, the fixed interest rate that was assumed despite market expectations of increased rates in the near future by the US Federal Reserve pushed the long-dated put options back up into the bid-ask spreads, resulting in these options being more accurately priced than the long-dated call options for all models.

7 Future Research

There are a number of ways the option pricing algorithm developed in this paper could be improved. To improve the regression of the expected continuation value, placement of knots could be explored. This could be done by either using an optimizer or by placing the knots in a fixed but not linear manner. To more accurately model the underlying stock movements, stochastic interest rates could be implemented as the fixed rates used in this report does not accurately represent the real financial markets. A simpler and perhaps equally efficient approach could be to implement a variable but deterministic interest rate that is said to e.g. increase by 0.25% every 6 months. Another improvement could be to find separate optimal model parameter values for different lengths of maturity, as some fixed parameters are bound to change over time.

Including crash dynamics and stochastic volatilities into the stock dynamics proved efficient for the pricing accuracies. Exploring models with both of these characteristics could therefore provide a greater pricing accuracy. Finally, it would be interesting to explore how a different underlying asset as well as a different time period, without the turbulence seen in spring 2022, could impact the results.

8 Appendix

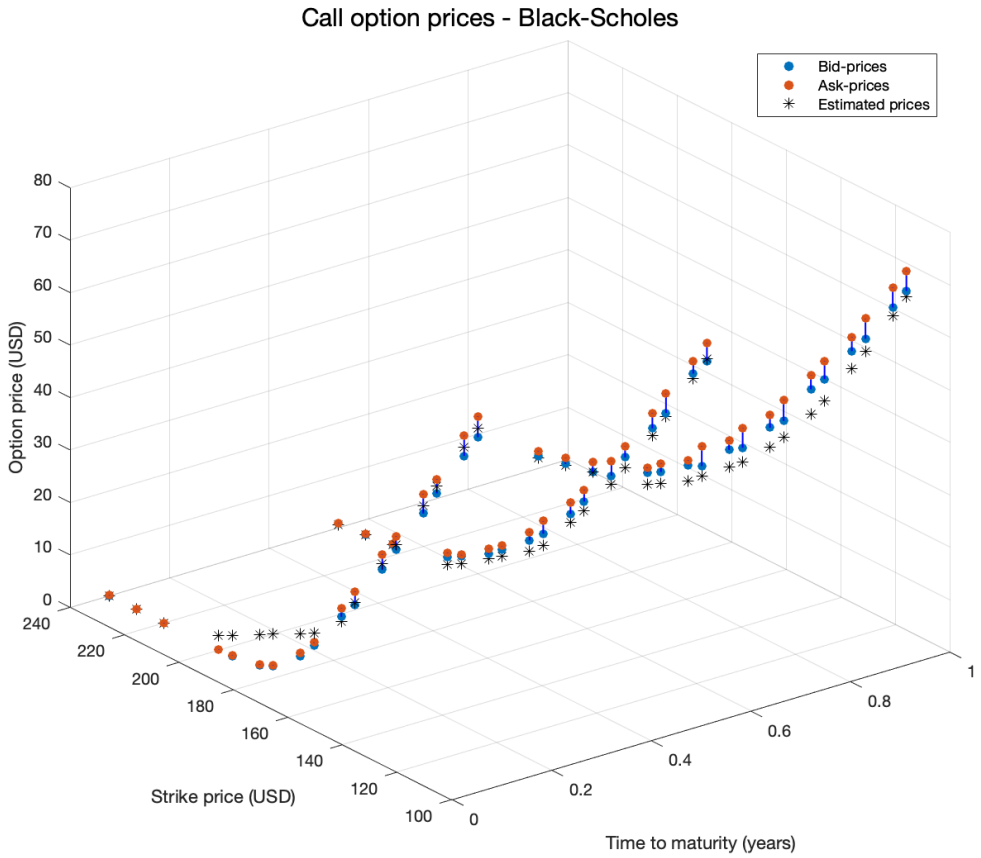

Figure 10: Estimated American option prices using Black-Scholes stock dynamics compared to bid and ask prices observed before market opening on 2022-04-08. Estimate achieved using a degree of 1 as a parameter for the SLM regression, resulting in an unwanted linear behaviour for the prices of the options with shortest maturity.

K \T	2022-07-15				2022-10-21				2023-01-20			
	$\hat{P}$	$\hat{P}_{zero}$	Bid	Ask	$\hat{P}$	$\hat{P}_{zero}$	Bid	Ask	$\hat{P}$	$\hat{P}_{zero}$	Bid	Ask
105	0.00	0.00	0.36	0.40	0.03	0.03	1.12	1.21	0.17	0.18	1.86	1.99
110	0.00	0.01	0.46	0.67	0.08	0.08	1.40	1.48	0.25	0.25	2.05	2.49
120	0.01	0.02	0.67	0.96	0.28	0.28	2.12	2.24	0.82	0.84	2.90	3.40
125	0.04	0.03	0.96	1.19	0.48	0.47	2.26	3.15	1.23	1.24	3.80	4.25
135	0.28	0.27	1.50	1.71	1.44	1.45	3.75	4.00	2.58	2.64	5.50	5.70
140	0.57	0.57	1.98	2.17	2.12	2.13	4.30	4.85	3.57	3.60	6.35	6.65
150	1.63	1.64	3.50	3.60	4.07	4.09	6.35	7.10	6.24	6.19	8.95	9.30
155	2.55	2.58	4.40	4.65	5.54	5.58	7.10	8.40	8.11	8.01	10.35	10.90
165	5.66	5.69	7.15	7.50	9.45	9.51	11.15	12.55	11.99	12.04	14.00	14.65
170	7.94	7.98	9.05	9.35	11.86	11.90	13.55	13.90	14.21	13.65	15.90	17.30
180	13.79	13.84	13.50	14.60	17.53	17.54	17.95	19.95	20.38	21.29	21.25	22.80
185	17.27	17.32	16.60	17.80	20.75	20.79	20.00	24.00	23.73	24.27	23.50	25.45
195	25.16	25.23	23.75	25.40	27.90	28.08	27.35	29.35	30.46	30.23	30.00	31.70
200	29.48	29.56	29.15	29.85	31.81	32.05	30.90	32.60	34.04	34.02	32.45	34.75
220	48.18	48.32	46.65	49.75	49.28	49.54	47.35	50.75	50.77	51.10	48.55	51.35
230	57.95	58.13	56.65	59.50	58.75	58.99	57.20	59.45	59.78	60.26	57.80	60.80
240	67.81	68.04	65.70	69.60	68.48	68.77	66.00	69.80	69.36	69.81	67.10	70.10

Table 9: Estimated put option values using stock trajectories simulated from Black-Scholes stock dynamics compared with observed bid and ask prices. $\hat{P}$ represents the estimates obtained with assumptions on the regressed curves. $\hat{P}_{zero}$ represents the estimates obtained when no assumptions are imposed.

K \T	2022-07-15				2022-10-21				2023-01-20			
	$\hat{C}$	$\hat{C}_{zero}$	Bid	Ask	$\hat{C}$	$\hat{C}_{zero}$	Bid	Ask	$\hat{C}$	$\hat{C}_{zero}$	Bid	Ask
105	67.34	67.44	66.00	69.00	67.59	67.92	67.10	70.50	67.77	68.11	68.70	71.70
110	62.36	62.53	61.20	64.00	62.64	62.90	63.40	65.70	62.96	63.12	64.20	67.30
120	52.38	52.49	51.85	54.40	52.79	52.70	53.30	56.95	53.43	53.42	55.70	58.50
125	47.39	47.52	47.70	49.70	47.90	48.25	49.05	52.00	48.80	49.15	51.35	53.95
135	37.45	37.54	38.10	40.55	38.43	38.22	40.90	43.05	39.55	39.63	42.85	45.15
140	32.66	32.71	34.20	36.05	34.27	34.09	36.10	38.85	35.23	35.28	38.70	42.50
150	23.96	23.97	25.65	27.35	26.89	27.25	28.55	30.75	28.34	28.70	31.40	33.60
155	20.13	20.14	21.55	23.25	23.33	23.55	24.90	27.00	25.26	25.41	28.40	30.35
165	13.51	13.54	14.60	15.10	16.89	16.71	18.50	20.90	19.82	19.74	22.25	23.90
170	10.72	10.74	11.55	11.85	14.19	14.05	15.90	17.50	17.22	17.96	19.60	21.15
180	6.23	6.22	6.60	6.85	9.85	9.99	11.55	12.25	12.30	11.70	15.35	15.95
185	4.53	4.52	4.75	5.00	8.20	8.38	9.40	10.35	10.33	9.92	13.00	13.75
195	2.23	2.22	2.44	2.51	5.71	5.75	6.30	6.60	7.68	7.93	9.45	10.70
200	1.53	1.54	1.63	1.78	4.75	4.70	4.85	5.75	6.78	6.92	8.10	8.65
220	0.41	0.46	0.34	0.42	1.96	1.91	2.03	2.19	3.55	3.50	4.05	4.35
230	0.26	0.29	0.20	0.24	1.10	1.14	1.26	1.38	2.36	2.33	2.81	3.05
240	0.17	0.14	0.12	0.15	0.57	0.64	0.80	0.90	1.65	1.72	1.96	2.16

Table 10: Estimated call option values using stock trajectories simulated from Black-Scholes stock dynamics compared with observed bid and ask prices. $\hat{C}$ represents the estimates obtained with assumptions on the regressed curves. $\hat{C}_{zero}$ represents the estimates obtained when no assumptions are imposed.

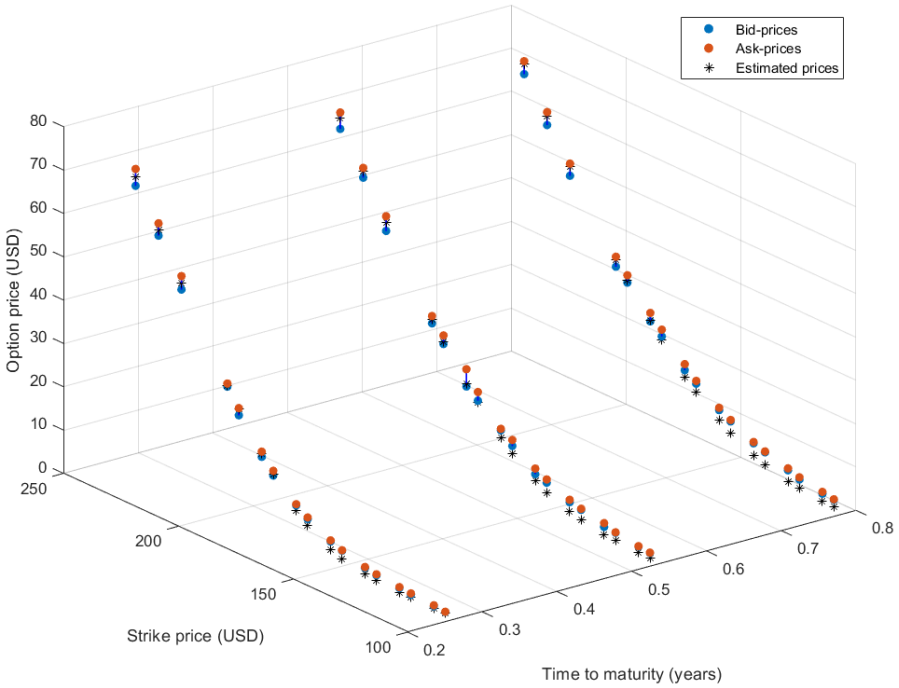

Figure 11: Estimated American put option prices using Black-Scholes stock dynamics compared to bid and ask prices observed before market opening on 2022-04-08.

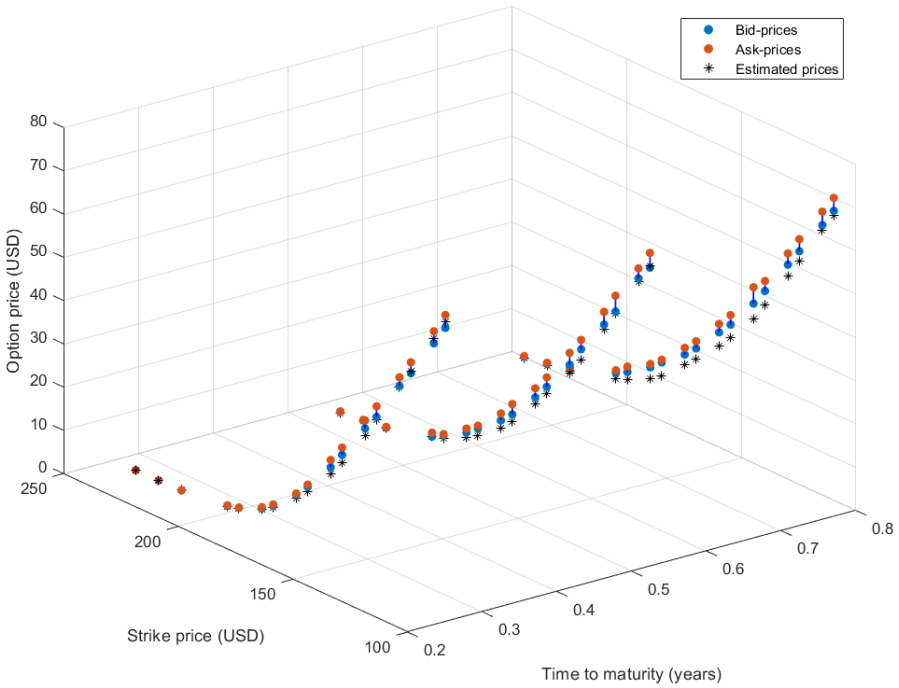

Figure 12: Estimated American call option prices using Black-Scholes stock dynamics compared to bid and ask prices observed before market opening on 2022-04-08.

K \T	2022-07-15				2022-10-21				2023-01-20			
	$\hat{P}$	$\hat{P}_{zero}$	Bid	Ask	$\hat{P}$	$\hat{P}_{zero}$	Bid	Ask	$\hat{P}$	$\hat{P}_{zero}$	Bid	Ask
105	0.26	0.28	0.36	0.40	0.93	0.93	1.12	1.21	1.60	1.65	1.86	1.99
110	0.34	0.32	0.46	0.67	1.15	1.19	1.40	1.48	1.99	2.02	2.05	2.49
120	0.77	0.79	0.67	0.96	1.84	1.82	2.12	2.24	3.10	3.19	2.90	3.40
125	1.16	1.17	0.96	1.19	2.50	2.54	2.26	3.15	3.74	3.67	3.80	4.25
135	2.32	2.29	1.50	1.71	4.14	4.15	3.75	4.00	5.50	5.23	5.50	5.70
140	3.03	3.00	1.98	2.17	5.11	5.08	4.30	4.85	6.80	7.02	6.35	6.65
150	4.48	4.50	3.50	3.60	7.56	7.61	6.35	7.10	9.69	9.53	8.95	9.30
155	5.21	5.27	4.40	4.65	8.97	9.00	7.10	8.40	11.50	11.81	10.35	10.90
165	6.82	6.96	7.15	7.50	12.16	12.13	11.15	12.55	15.30	15.28	14.00	14.65
170	8.11	8.25	9.05	9.35	13.96	13.97	13.55	13.90	17.29	17.53	15.90	17.30
180	12.64	12.63	13.50	14.60	18.16	18.24	17.95	19.95	22.00	21.88	21.25	22.80
185	15.97	15.82	16.60	17.80	20.62	20.70	20.00	24.00	24.82	24.73	23.50	25.45
195	24.04	23.70	23.75	25.40	26.63	26.68	27.35	29.35	31.02	31.25	30.00	31.70
200	28.53	28.19	29.15	29.85	30.30	30.35	30.90	32.60	34.26	34.54	32.45	34.75
220	47.74	48.15	46.65	49.75	48.30	48.50	47.35	50.75	49.28	49.77	48.55	51.35
230	57.74	58.46	56.65	59.50	58.09	58.39	57.20	59.45	58.76	59.20	57.80	60.80
240	67.74	68.55	65.70	69.60	67.99	68.37	66.00	69.80	68.39	68.13	67.10	70.10

Table 11: Estimated put option values using stock trajectories simulated from Merton stock dynamics compared with observed bid and ask prices. $\hat{P}$ represents the estimates obtained with assumptions on the regressed curves. $\hat{P}_{zero}$ represents the estimates obtained when no assumptions are imposed.

K \T	2022-07-15				2022-10-21				2023-01-20			
	$\hat{C}$	$\hat{C}_{zero}$	Bid	Ask	$\hat{C}$	$\hat{C}_{zero}$	Bid	Ask	$\hat{C}$	$\hat{C}_{zero}$	Bid	Ask
105	67.35	67.36	66.00	69.00	67.99	68.08	67.10	70.50	68.61	69.38	68.70	71.70
110	62.45	62.66	61.20	64.00	63.40	63.43	63.40	65.70	64.07	64.16	64.20	67.30
120	53.00	53.05	51.85	54.40	54.54	54.37	53.30	56.95	55.31	55.84	55.70	58.50
125	48.36	48.33	47.70	49.70	50.11	49.93	49.05	52.00	50.96	50.43	51.35	53.95
135	39.54	39.40	38.10	40.55	41.32	41.33	40.90	43.05	42.99	43.77	42.85	45.15
140	35.33	35.19	34.20	36.05	37.21	37.19	36.10	38.85	39.11	38.69	38.70	42.50
150	26.97	27.06	25.65	27.35	29.94	30.08	28.55	30.75	32.44	32.82	31.40	33.60
155	22.79	23.00	21.55	23.25	26.55	26.64	24.90	27.00	29.28	29.09	28.40	30.35
165	14.58	14.77	14.60	15.10	19.96	19.87	18.50	20.90	23.03	23.22	22.25	23.90
170	10.92	11.01	11.55	11.85	16.73	16.66	15.90	17.50	20.09	20.13	19.60	21.15
180	5.44	5.28	6.60	6.85	10.96	10.97	11.55	12.25	15.03	14.93	15.35	15.95
185	3.69	3.42	4.75	5.00	8.59	8.62	9.40	10.35	12.80	12.81	13.00	13.75
195	1.58	1.18	2.44	2.51	4.91	4.92	6.30	6.60	8.54	8.54	9.45	10.70
200	0.99	0.58	1.63	1.78	3.56	3.56	4.85	5.75	6.65	6.55	8.10	8.65
220	0.06	0.00	0.34	0.42	0.71	0.67	2.03	2.19	2.33	2.36	4.05	4.35
230	0.00	0.04	0.20	0.24	0.22	0.21	1.26	1.38	1.24	1.21	2.81	3.05
240	0.00	0.10	0.12	0.15	0.04	0.07	0.80	0.90	0.58	0.59	1.96	2.16

Table 12: Estimated call option values using stock trajectories simulated from Merton stock dynamics compared with observed bid and ask prices. $\hat{C}$ represents the estimates obtained with assumptions on the regressed curves. $\hat{C}_{zero}$ represents the estimates obtained when no assumptions are imposed.

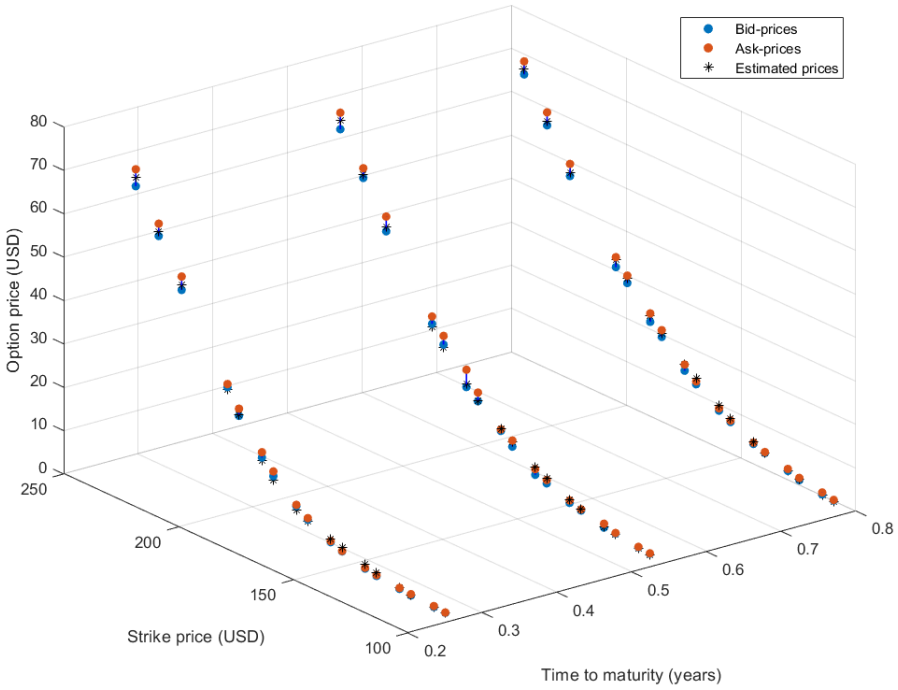

Figure 13: Estimated American put option prices using Merton Jump Diffusion stock dynamics compared to bid and ask prices observed before market opening on 2022-04-08.

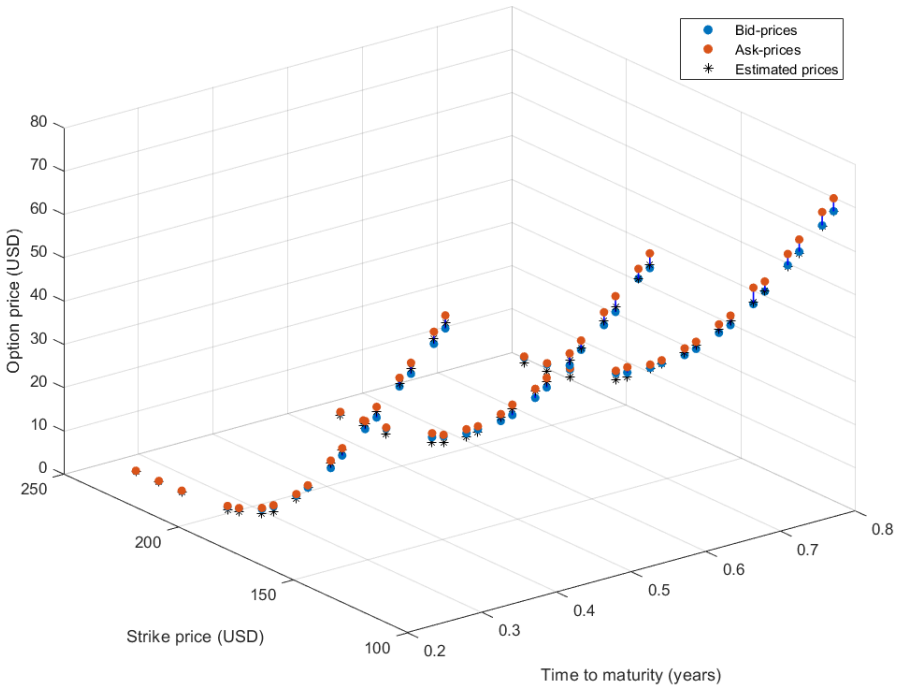

Figure 14: Estimated American put option prices using Merton Jump Diffusion stock dynamics compared to bid and ask prices observed before market opening on 2022-04-08.

K \T	2022-07-15				2022-10-21				2023-01-20			
	$\hat{P}$	$\hat{P}_{zero}$	Bid	Ask	$\hat{P}$	$\hat{P}_{zero}$	Bid	Ask	$\hat{P}$	$\hat{P}_{zero}$	Bid	Ask
105	0.26	0.28	0.36	0.40	0.93	0.93	1.12	1.21	1.60	1.65	1.86	1.99
110	0.34	0.32	0.46	0.67	1.15	1.19	1.40	1.48	1.99	2.02	2.05	2.49
120	0.77	0.79	0.67	0.96	1.84	1.82	2.12	2.24	3.10	3.19	2.90	3.40
125	1.16	1.17	0.96	1.19	2.50	2.54	2.26	3.15	3.74	3.67	3.80	4.25
135	2.32	2.29	1.50	1.71	4.14	4.15	3.75	4.00	5.50	5.23	5.50	5.70
140	3.03	3.00	1.98	2.17	5.11	5.08	4.30	4.85	6.80	7.02	6.35	6.65
150	4.48	4.50	3.50	3.60	7.56	7.61	6.35	7.10	9.69	9.53	8.95	9.30
155	5.21	5.27	4.40	4.65	8.97	9.00	7.10	8.40	11.50	11.81	10.35	10.90
165	6.82	6.96	7.15	7.50	12.16	12.13	11.15	12.55	15.30	15.28	14.00	14.65
170	8.11	8.25	9.05	9.35	13.96	13.97	13.55	13.90	17.29	17.53	15.90	17.30
180	12.64	12.63	13.50	14.60	18.16	18.24	17.95	19.95	22.00	21.88	21.25	22.80
185	15.97	15.82	16.60	17.80	20.62	20.70	20.00	24.00	24.82	24.73	23.50	25.45
195	24.04	23.70	23.75	25.40	26.63	26.68	27.35	29.35	31.02	31.25	30.00	31.70
200	28.53	28.19	29.15	29.85	30.30	30.35	30.90	32.60	34.26	34.54	32.45	34.75
220	47.74	48.15	46.65	49.75	48.30	48.50	47.35	50.75	49.28	49.77	48.55	51.35
230	57.74	58.46	56.65	59.50	58.09	58.39	57.20	59.45	58.76	59.20	57.80	60.80
240	67.74	68.55	65.70	69.60	67.99	68.37	66.00	69.80	68.39	68.13	67.10	70.10

Table 13: Estimated put option values using stock trajectories simulated from FMLS stock dynamics compared with observed bid and ask prices. $\hat{P}$ represents the estimates obtained with assumptions on the regressed curves. $\hat{P}_{zero}$ represents the estimates obtained when no assumptions are imposed.

K \T	2022-07-15				2022-10-21				2023-01-20			
	$\hat{C}$	$\hat{C}_{zero}$	Bid	Ask	$\hat{C}$	$\hat{C}_{zero}$	Bid	Ask	$\hat{C}$	$\hat{C}_{zero}$	Bid	Ask
105	67.93	67.64	66.00	69.00	68.54	68.35	67.10	70.50	69.31	69.88	68.70	71.70
110	63.08	62.96	61.20	64.00	63.86	64.61	63.40	65.70	64.66	64.40	64.20	67.30
120	53.41	53.58	51.85	54.40	54.59	54.01	53.30	56.95	55.57	54.94	55.70	58.50
125	48.57	48.58	47.70	49.70	50.04	49.86	49.05	52.00	51.22	50.64	51.35	53.95
135	38.97	38.89	38.10	40.55	41.03	41.38	40.90	43.05	42.75	42.14	42.85	45.15
140	34.33	34.29	34.20	36.05	36.65	36.56	36.10	38.85	38.55	37.98	38.70	42.50
150	25.62	25.59	25.65	27.35	28.66	28.38	28.55	30.75	31.27	31.32	31.40	33.60
155	21.57	21.54	21.55	23.25	25.05	25.03	24.90	27.00	27.88	27.38	28.40	30.35
165	14.18	14.21	14.60	15.10	18.52	18.72	18.50	20.90	21.57	21.93	22.25	23.90
170	10.98	11.04	11.55	11.85	15.62	15.73	15.90	17.50	18.66	18.16	19.60	21.15
180	5.96	6.04	6.60	6.85	10.68	10.58	11.55	12.25	14.04	14.52	15.35	15.95
185	4.24	4.28	4.75	5.00	8.67	8.55	9.40	10.35	11.96	12.11	13.00	13.75
195	2.06	1.98	2.44	2.51	5.50	5.46	6.30	6.60	8.55	8.38	9.45	10.70
200	1.42	1.28	1.63	1.78	4.29	4.30	4.85	5.75	7.20	7.38	8.10	8.65
220	0.28	0.08	0.34	0.42	1.44	1.49	2.03	2.19	3.11	3.00	4.05	4.35
230	0.09	0.00	0.20	0.24	0.80	0.81	1.26	1.38	2.19	2.29	2.81	3.05
240	0.02	0.00	0.12	0.15	0.43	0.40	0.80	0.90	1.43	1.40	1.96	2.16

Table 14: Estimated call option values using stock trajectories simulated from FMLS stock dynamics compared with observed bid and ask prices. $\hat{C}$ represents the estimates obtained with assumptions on the regressed curves. $\hat{C}_{zero}$ represents the estimates obtained when no assumptions are imposed.

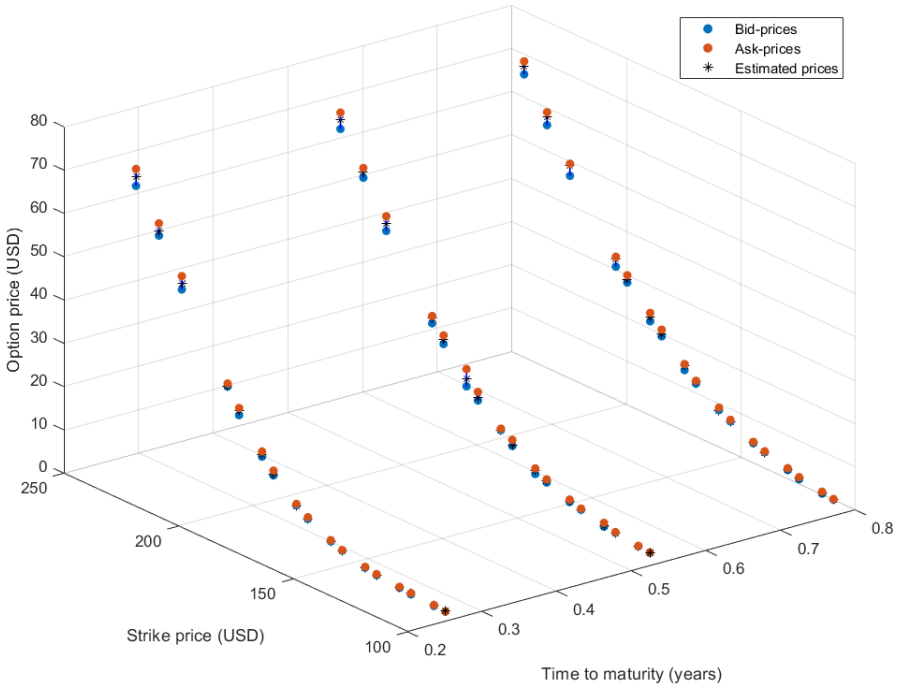

Figure 15: Estimated American put option prices using FMLS stock dynamics compared to bid and ask prices observed before market opening on 2022-04-08.

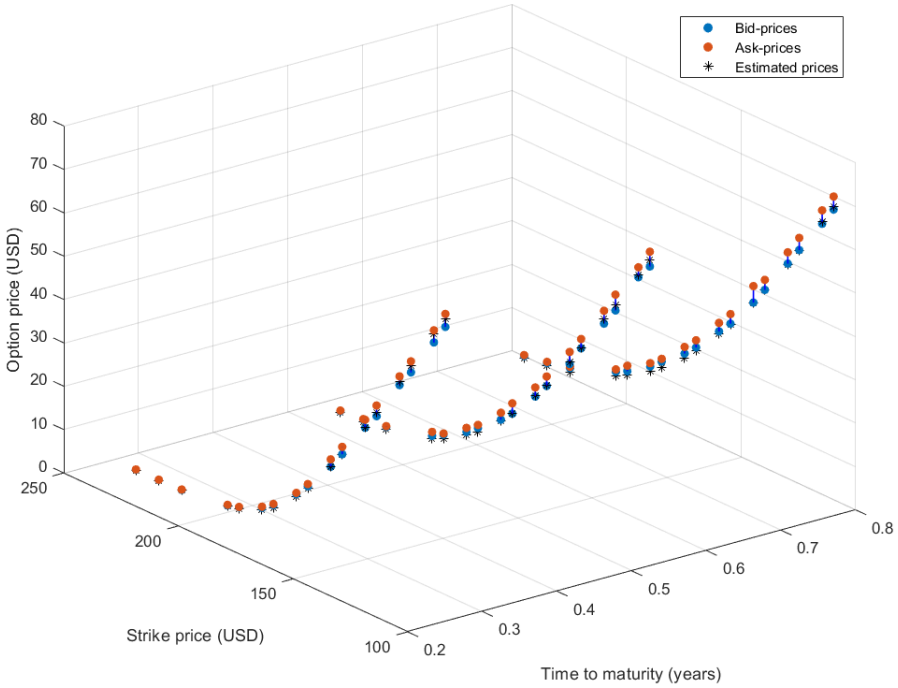

Figure 16: Estimated American call option prices using FMLS stock dynamics compared to bid and ask prices observed before market opening on 2022-04-08.

K \T	2022-07-15				2022-10-21				2023-01-20			
	$\hat{P}$	$\hat{P}_{zero}$	Bid	Ask	$\hat{P}$	$\hat{P}_{zero}$	Bid	Ask	$\hat{P}$	$\hat{P}_{zero}$	Bid	Ask
105	0.01	0.00	0.36	0.40	0.18	0.13	1.12	1.21	0.71	0.67	1.86	1.99
110	0.02	0.01	0.46	0.67	0.38	0.44	1.40	1.48	0.99	1.05	2.05	2.49
120	0.08	0.10	0.67	0.96	0.97	0.82	2.12	2.24	1.99	2.05	2.90	3.40
125	0.16	0.16	0.96	1.19	1.36	1.73	2.26	3.15	2.68	2.57	3.80	4.25
135	0.65	0.65	1.50	1.71	2.32	2.17	3.75	4.00	4.27	4.20	5.50	5.70
140	0.98	0.98	1.98	2.17	3.10	3.06	4.30	4.85	5.41	5.55	6.35	6.65
150	2.05	2.03	3.50	3.60	5.72	5.54	6.35	7.10	8.26	8.33	8.95	9.30
155	3.09	3.06	4.40	4.65	7.32	7.21	7.10	8.40	10.05	10.23	10.35	10.90
165	6.44	6.49	7.15	7.50	10.94	11.46	11.15	12.55	13.80	14.12	14.00	14.65
170	8.71	8.86	9.05	9.35	13.23	13.64	13.55	13.90	15.97	16.25	15.90	17.30
180	14.38	14.80	13.50	14.60	18.77	18.85	17.95	19.95	22.01	22.32	21.25	22.80
185	17.72	18.28	16.60	17.80	21.93	22.21	20.00	24.00	25.30	25.55	23.50	25.45
195	25.36	26.06	23.75	25.40	29.07	29.92	27.35	29.35	31.91	32.36	30.00	31.70
200	29.59	30.30	29.15	29.85	33.05	34.02	30.90	32.60	35.45	36.08	32.45	34.75
220	48.16	49.17	46.65	49.75	50.18	50.68	47.35	50.75	52.24	53.86	48.55	51.35
230	57.92	59.51	56.65	59.50	59.02	59.89	57.20	59.45	60.91	63.03	57.80	60.80
240	67.81	70.26	65.70	69.60	68.22	71.63	66.00	69.80	69.68	70.89	67.10	70.10

Table 15: Estimated put option values using stock trajectories simulated from Heston stock dynamics compared with observed bid and ask prices. $\hat{P}$ represents the estimates obtained with assumptions on the regressed curves. $\hat{P}_{zero}$ represents the estimates obtained when no assumptions are imposed.

K \T	2022-07-15				2022-10-21				2023-01-20			
	$\hat{C}$	$\hat{C}_{zero}$	Bid	Ask	$\hat{C}$	$\hat{C}_{zero}$	Bid	Ask	$\hat{C}$	$\hat{C}_{zero}$	Bid	Ask
105	67.48	68.68	66.00	69.00	68.42	69.52	67.10	70.50	68.69	70.65	68.70	71.70
110	62.57	63.32	61.20	64.00	63.57	63.96	63.40	65.70	63.78	64.17	64.20	67.30
120	52.76	53.15	51.85	54.40	53.87	53.90	53.30	56.95	54.27	54.82	55.70	58.50
125	47.86	48.37	47.70	49.70	49.14	49.14	49.05	52.00	49.75	51.40	51.35	53.95
135	38.16	37.80	38.10	40.55	40.82	40.78	40.90	43.05	41.54	42.79	42.85	45.15
140	33.56	32.87	34.20	36.05	36.82	36.57	36.10	38.85	37.72	38.68	38.70	42.50
150	25.09	24.70	25.65	27.35	28.82	28.76	28.55	30.75	30.27	30.56	31.40	33.60
155	21.15	20.97	21.55	23.25	24.82	24.86	24.90	27.00	26.98	27.05	28.40	30.35
165	14.02	14.00	14.60	15.10	17.72	17.69	18.50	20.90	21.44	21.70	22.25	23.90
170	11.01	10.99	11.55	11.85	15.19	15.37	15.90	17.50	19.07	19.22	19.60	21.15
180	6.34	6.28	6.60	6.85	11.31	11.68	11.55	12.25	14.61	14.66	15.35	15.95
185	4.63	4.55	4.75	5.00	9.52	9.59	9.40	10.35	12.46	12.43	13.00	13.75
195	2.28	2.22	2.44	2.51	6.32	5.82	6.30	6.60	8.99	8.95	9.45	10.70
200	1.58	1.55	1.63	1.78	5.03	4.57	4.85	5.75	7.67	7.71	8.10	8.65
220	0.43	0.45	0.34	0.42	1.74	1.84	2.03	2.19	3.54	3.56	4.05	4.35
230	0.24	0.14	0.20	0.24	0.92	0.83	1.26	1.38	2.44	2.34	2.81	3.05
240	0.14	0.00	0.12	0.15	0.43	0.26	0.80	0.90	1.76	1.83	1.96	2.16

Table 16: Estimated call option values using stock trajectories simulated from Heston stock dynamics compared with observed bid and ask prices. $\hat{C}$ represents the estimates obtained with assumptions on the regressed curves. $\hat{C}_{zero}$ represents the estimates obtained when no assumptions are imposed.

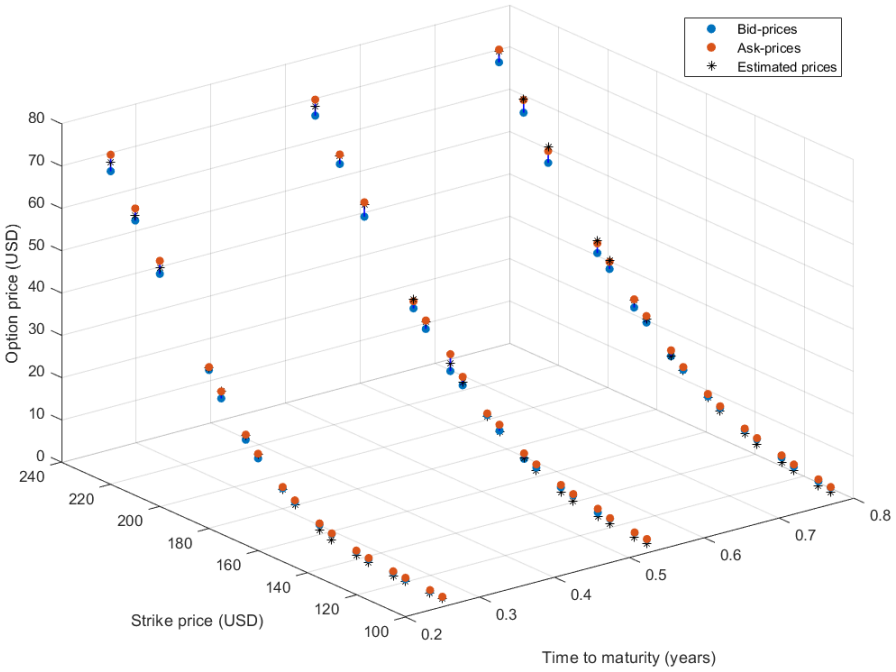

Figure 17: Estimated American put option prices using Heston stock dynamics compared to bid and ask prices observed before market opening on 2022-04-08.

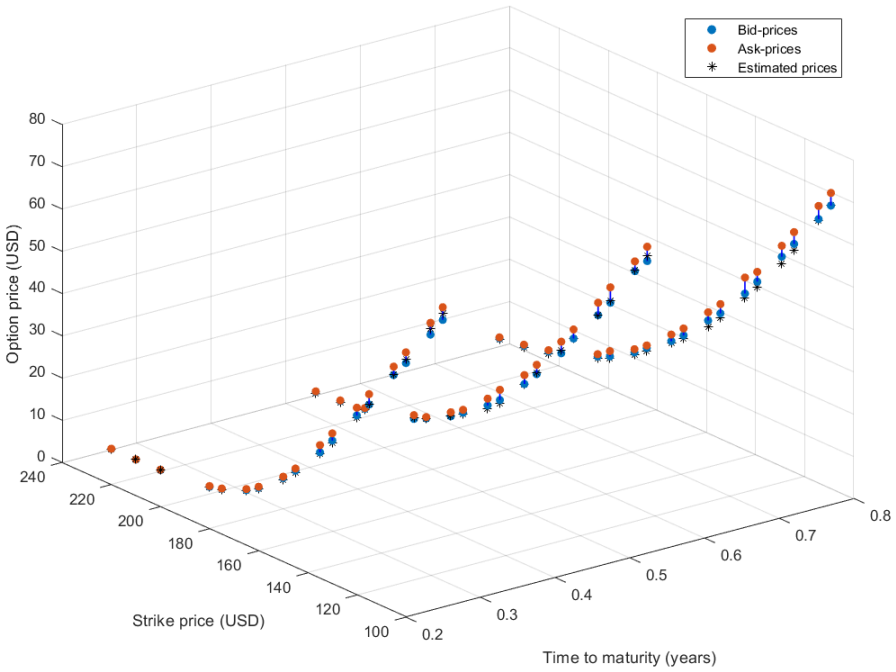

Figure 18: Estimated American call option prices using Heston stock dynamics compared to bid and ask prices observed before market opening on 2022-04-08.

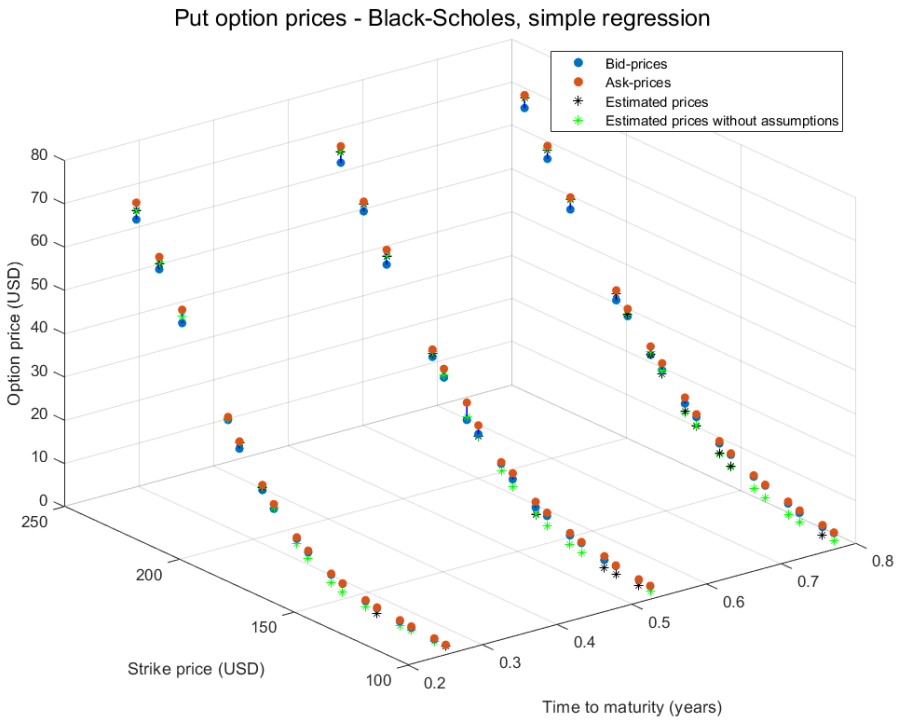

Figure 19: Estimated American put option prices using Black-Scholes stock dynamics compared to bid and ask prices observed before market opening on 2022-04-08. The green points represent option price estimations found without using assumptions in the regression of the expected continuation function.

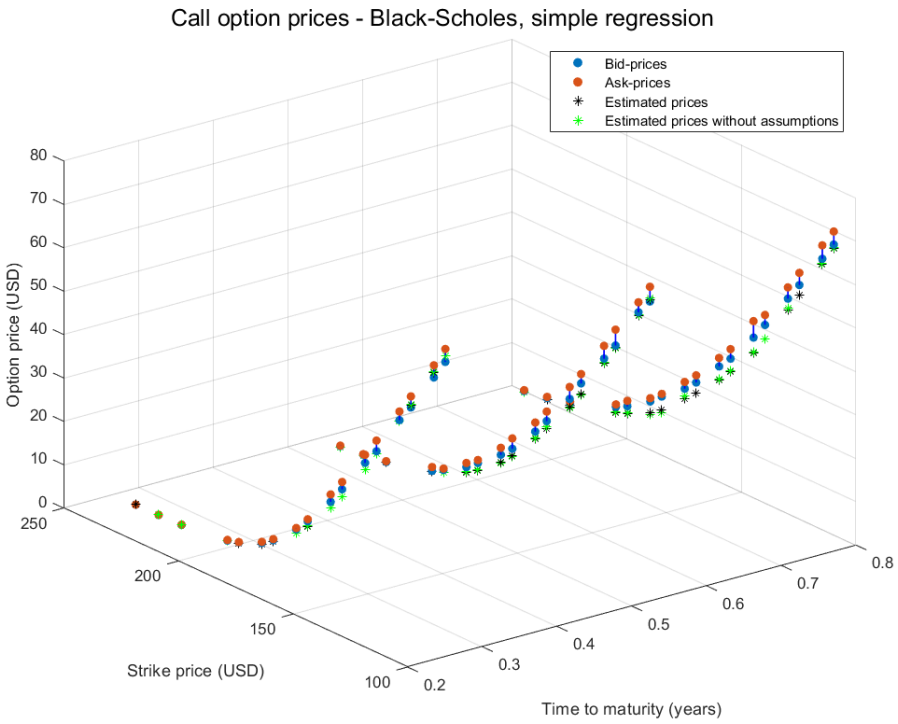

Figure 20: Estimated American put option prices using Black-Scholes stock dynamics compared to bid and ask prices observed before market opening on 2022-04-08. The green points represent option price estimations found without using assumptions in the regression of the expected continuation function.

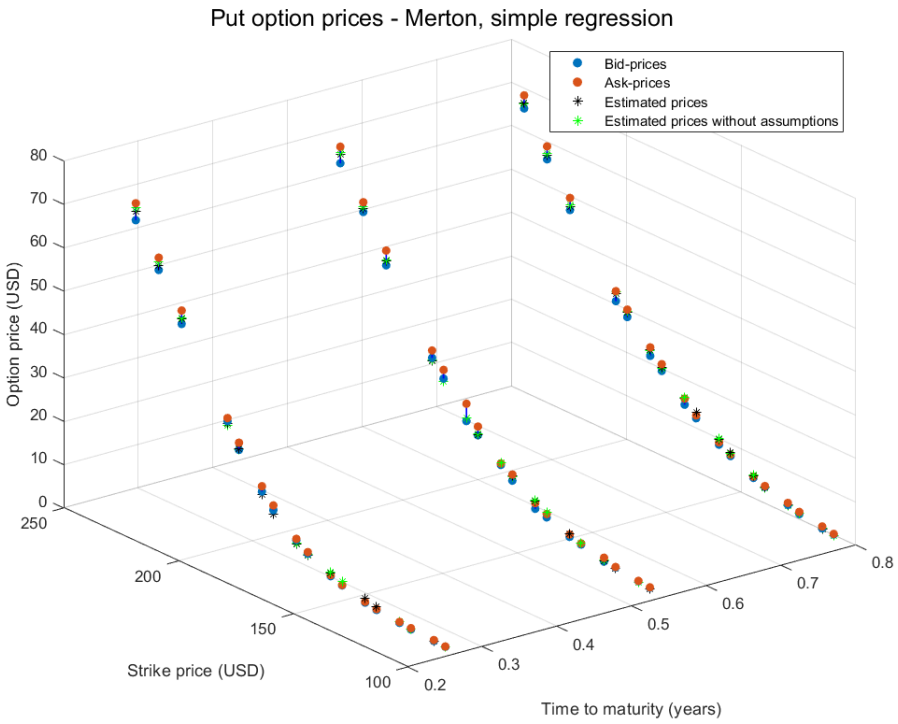

Figure 21: Estimated American put option prices using Merton Jump Diffusion stock dynamics compared to bid and ask prices observed before market opening on 2022-04-08. The green points represent option price estimations found without using assumptions in the regression of the expected continuation function.

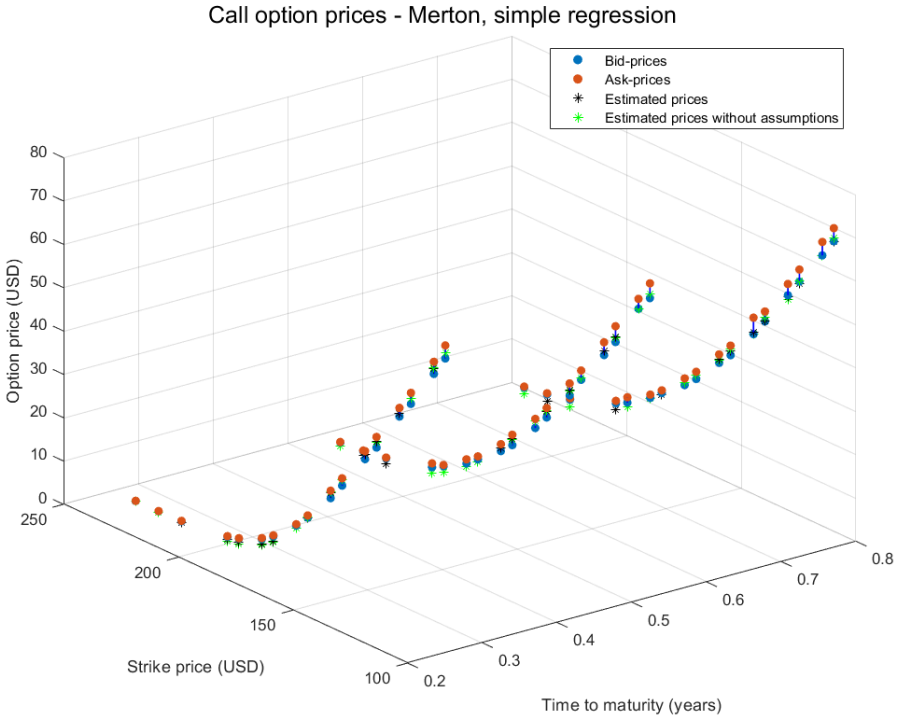

Figure 22: Estimated American call option prices using Merton Jump Diffusion stock dynamics compared to bid and ask prices observed before market opening on 2022-04-08. The green points represent option price estimations found without using assumptions in the regression of the expected continuation function.

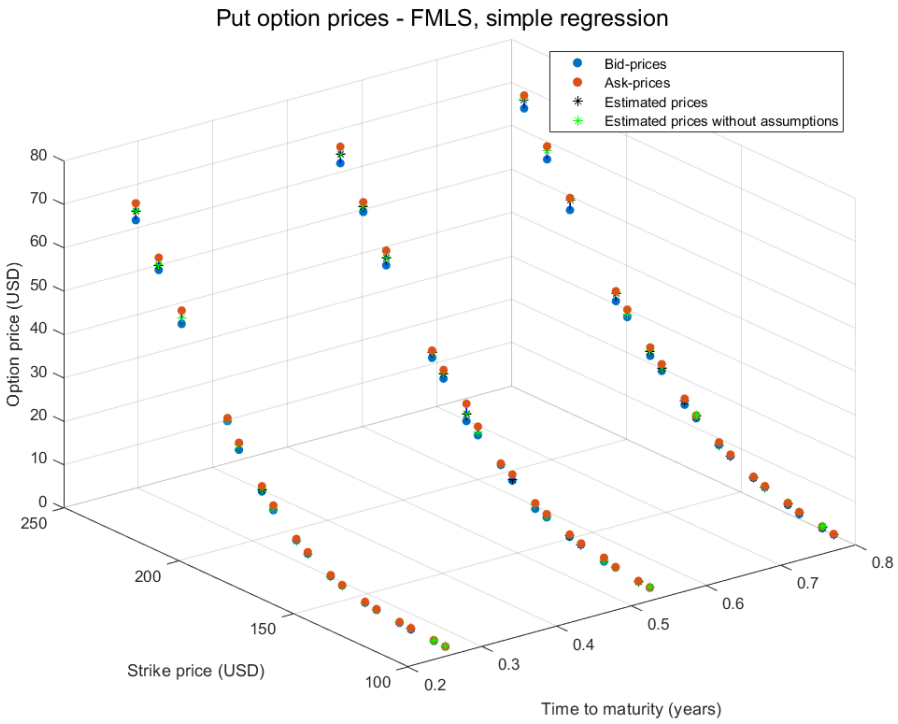

Figure 23: Estimated American put option prices using FMLS stock dynamics compared to bid and ask prices observed before market opening on 2022-04-08. The green points represent option price estimations found without using assumptions in the regression of the expected continuation function.

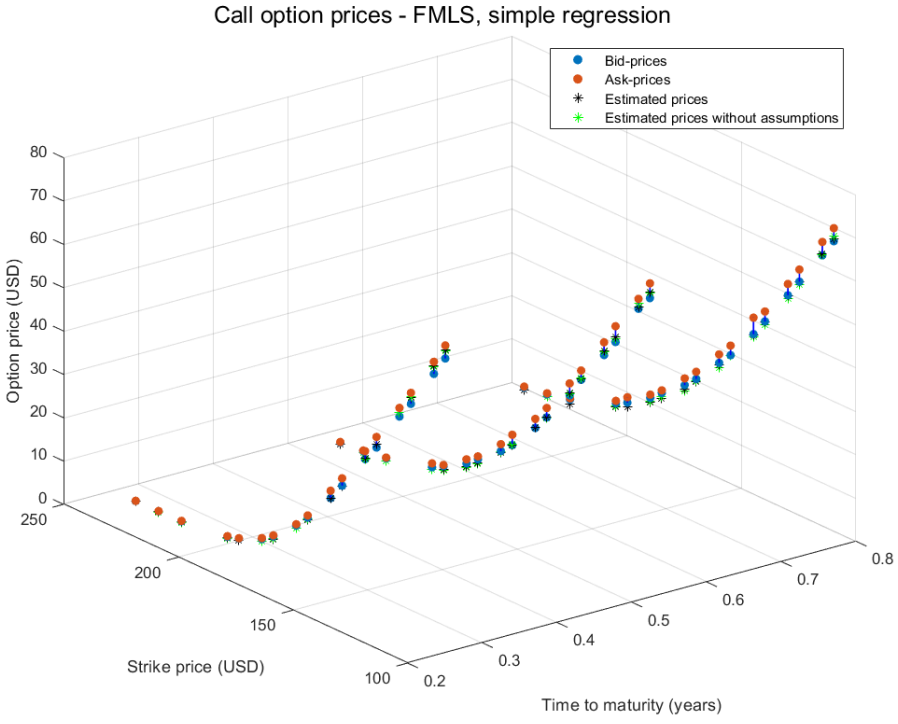

Figure 24: Estimated American call option prices using FMLS stock dynamics compared to bid and ask prices observed before market opening on 2022-04-08. The green points represent option price estimations found without using assumptions in the regression of the expected continuation function.

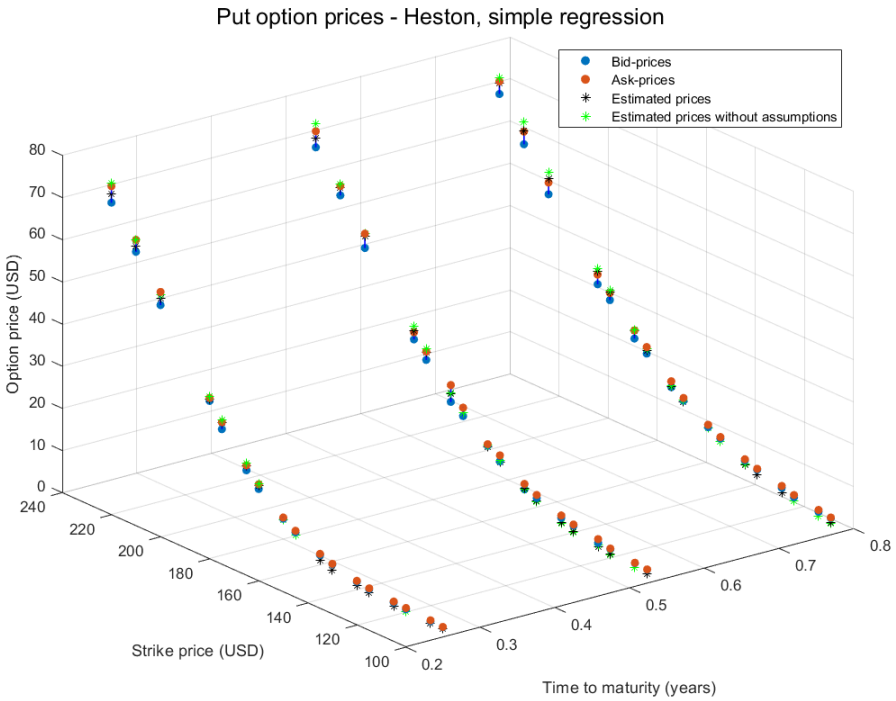

Figure 25: Estimated American put option prices using Heston stock dynamics compared to bid and ask prices observed before market opening on 2022-04-08. The green points represent option price estimations found without using assumptions in the regression of the expected continuation function.

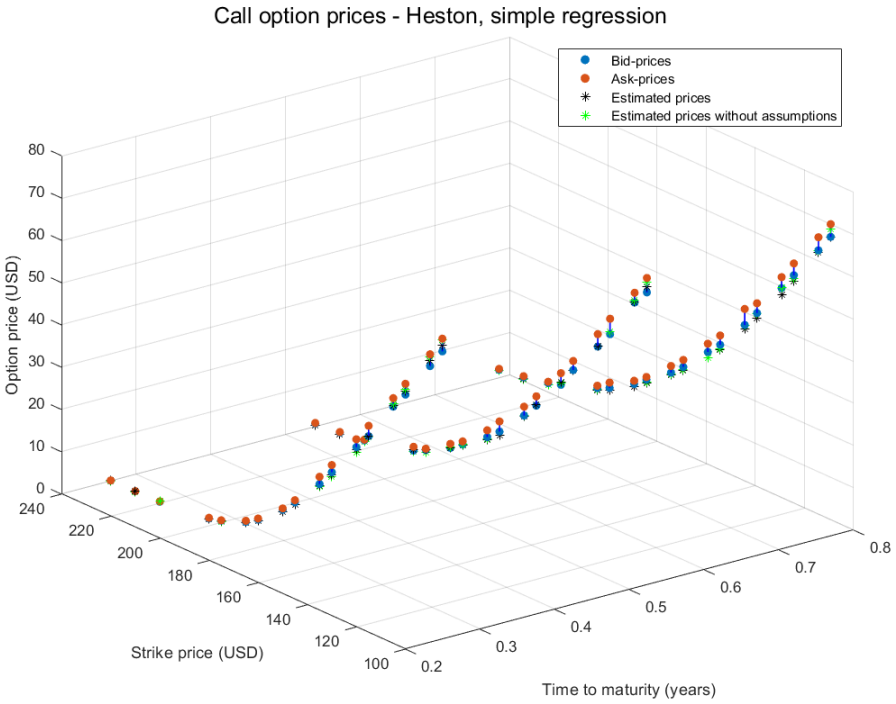

Figure 26: Estimated American call option prices using Heston stock dynamics compared to bid and ask prices observed before market opening on 2022-04-08. The green points represent option price estimations found without using assumptions in the regression of the expected continuation function.

References

[1] Björk, T. *Arbitrage Theory in Continuous Time*, pages 67–69, 92–112. 2009.

[2] Black, F., Scholes, M. The Pricing of Options and Corporate Liabilities. *Journal of Political Economy*, **81**:637–654, 1973.

[3] Carr, P., Wu, L. The Finite Moment Log Stable Process and Option Pricing. *The Journal Of Finance*, **58**:753–776, 2003.

[4] D'Errico, J. SLM - Shape Language Modeling, 2022.

[5] Givens, G. H., Hoeting, J. A. *Computational Statistics*, pages 13–14, 151–153. 2013.

[6] Heston, S. L. A Closed Form Solution for Options with Stochastic Volatility with Applications to Bond and Currency Options. *The Review of Financial Studies*, **6**:327–343, 1993.

[7] Jain, S., Oosterlee, C. W. The Stochastic Grid Bundling Method: Efficient pricing of bermudan options and their greeks. *Applied Mathematics and Computation*, **269**:412–431, 2015.

[8] Longstaff, F., Schwartz, E. Valuing American Options by Simulation: A simple least- squares approach. *The Review of Financial Studies*, **14**:113–147, 2001.

[9] Merton, R. C. Option Pricing when Underlying Stock Returns are Discontinuous. *Journal of Financial Economics*, **3**:125–144, 1976.

[10] The MathWorks, Inc. MATLAB Global Optimization Toolbox, 2022.

[11] Campbell, R. The volatility index: Reading market sentiment. URL: https://www.investopedia.com/articles/optioninvestor/09/implied-volatility-contrary-indicator.asp.

[12] Ganti, A. Implied volatility. URL: https://www.investopedia.com/terms/i/iv.asp.

[13] Hayes, A. Guide to dividends. URL: https://www.investopedia.com/terms/d/dividend.asp#:~:text=A%20dividend%20is%20the%20distribution%20of%20corporate%20profits%20to%20eligible,their%20money%20into%20the%20venture.

[14] Seth, S. How and why interest rates affect options. URL: https://www.investopedia.com/articles/active-trading/051415/how-why-interest-rates-affect-options.asp#:~:text=With%20an%20increase%20in%20interest,negatively%20by%20increasing%20interest%20rates.

[15] Smith, C. Expectations grow that fed will deploy jumbo-size rate rises. *Financial Times*. URL: https://www.ft.com/content/56830aa5-be37-4ebc-808a-64c6ad4ce670.

[16] 3 Month Treasury Bill Rate. URL: https://ycharts.com/indicators/3_month_t_bill#:~:text=3%20Month%20Treasury%20Bill%20Rate%20is%20at%200.67%25%2C%20compared%20to,long%20term%20average%20of%204.19%25.

[17] Apple Dividend History. URL: https://investor.apple.com/dividend-history/default.aspx.

[18] Apple Options Delayed Quotes. URL: https://www.cboe.com/delayed_quotes/aapl.

[19] Apple Stock Price. URL: https://investor.apple.com/stock-price/default.aspx.

[20] CBOE Volatility Index: Historical prices. URL: https://www.wsj.com/market-data/quotes/index/VIX/historical-prices.

[21] U.S. Equity and Options Markets Holiday Schedule 2022. URL: http://www.nasdaqtrader.com/trader.aspx?id=calendar.